Available online at www.sciencedirect.com
ScienceDirect
Spectrochimica Acta Part A 69 (2008) 1027–1043
SPECTROCHIMICA ACTA PART A
www.elsevier.com/locate/saa

DFT calculation of the chromyl nitrate, $CrO_2(NO_3)_2$ The molecular force field

S.A. Brandán, M.L. Roldán, C. Socolsky, A. Ben Altabef *,[1]

Cátedra de Fisicoquímica I, Instituto de Química Física, Facultad de Bioquímica, Química y Farmacia, Universidad Nacional de Tucumán, San Lorenzo 456, T4000CAN Tucumán, Argentina

Received 28 December 2006; accepted 2 June 2007

Abstract

We have carried out a structural and vibrational theoretical study for chromyl nitrate. The density functional theory has been used to study its structure and vibrational properties. The geometries were fully optimised at the B3LYP/Lanl2DZ, B3LYP/6-31G* and B3LYP/6-311++G levels of theory and the harmonic vibrational frequencies were evaluated at the same levels. The calculated harmonic vibrational frequencies for chromyl nitrate are consistent with the experimental IR and Raman spectra in the solid and liquid phases. These calculations gave us a precise knowledge of the normal modes of vibration taking into account the type of coordination adopted by nitrate groups of this compound as monodentate and bidentate. We have also made the assignment of all the observed bands in the vibrational spectra for chromyl nitrate. The nature of the Cr–O and Cr ← O bonds in the compound were quantitatively investigated by means of Natural Bond Order (NBO) analysis. The topological properties of electronic charge density are analysed employing Bader's Atoms in Molecules theory (AIM).

Keywords: $CrO_2(NO_3)_2$; Coordination monodentate; Coordination bidentate; DFT; Vibrational spectra; Theoretical study; Molecular geometry; Force field

1. Introduction

The study of compounds that contains transition metals, such as V and Cr [1–6] is of great interest in our laboratory. The compounds with the nitrate group as ligand are particularly interesting because this group is a versatile ligand and can act as monodentate or bidentate ligand [7]. The mode of coordination adopted by nitrate groups and the stereochemistry of this compound are important in relation to the vibrational properties and chemical reactivity [8–10]. The chromyl nitrate, $CrO_2(NO_3)_2$, compound presents vibrational properties imperfectly described and only the main characteristics of the infrared spectrum were published in liquid phase [11] and in previous studies we have assigned some bands observed in the vibrational spectra of the chromyl nitrate [1]. Marsden et al. have studied the gas-phase molecular structure of chromyl nitrate, $CrO_2(NO_3)_2$, by electron diffraction at a temperature of 50 °C and by *ab initio* methods at the HF level [12]. In this case the diffraction data are consistent with C_2 symmetry for the molecule. The Cr coordination is best described as derived from a severely distorted octahedron, since the nitrate group's act as bidentate ligands which are asymmetrically bonded to Cr.

This dark red liquid compound, can be obtained by several methods [11–16] and it is very reactive at room temperature but less unstable than other compounds with the chromyl group [17,18]. The aim of this work is to carry out an experimental and theoretical study on this compound with the methods of quantum chemistry in order to have a better understanding of its vibrational properties. A precise knowledge of the normal modes of vibration is expected to provide a foundation for understanding the conformation-sensitive bands in vibrational spectra of this molecule. In this case the normal mode calculations were accomplished using a generalized valence force field (GVFF) and considering the nitrate group as monodentate and bidentate ligand. In the present work we have performed an experimental and theoretical study of chromyl nitrate, $CrO_2(NO_3)_2$, in order to study the coordination mode of nitrate groups and carry out its complete assignment. For that purpose, the optimised geometry and frequencies for the normal modes of vibration were calculated. In this case, there are no publications about experimental

* Corresponding author. Tel.: +54 381 4311044; fax: +54 381 4248169.
E-mail address: altabef@fbqf.unt.edu.ar (A. Ben Altabef).
[1] A. Ben Altabef is member of the Research Career of CONICET (National Research Council of R. Argentina).

1386-1425/$ – see front matter © 2007 Elsevier B.V. All rights reserved.
doi:10.1016/j.saa.2007.06.020

or high-level theoretical studies on the geometries and force field of chromyl nitrate. Hence, obtaining reliable parameters by theoretical methods is an appealing alternative. The parameters obtained may be used to gain chemical and vibrational insights into related compounds. The election of the method and the basis sets are very important to evaluate not only the best level of theory but also the best basis set to be used to reproduce the experimental geometry and the vibrational frequencies. In previous studies of compounds that contain metal transition such as $VO_2X_2^-$ (X = F, Cl) anions [3] the HF and MP2 methodologies are much less satisfactory than the DFT techniques specially for the V–Cl distance. In this case the basis set that best reproduces the experimental geometrical parameters for the chloro compound is B3PW91/6-311G* while the inclusion of polarization functions is important to have a better agreement. In the VOX_3 (X = F, Cl, Br, I) series the optimised geometry which better reproduces the experimental parameters was obtained with the B3PW91/6-311G calculation while the B3LYP method produces the best results for the vibrational frequencies [4]. In a recent paper about oxotetrachlorochromate (V) anion [6] it was found that the inclusion of polarization functions in the basis sets significantly improved the theoretical geometry results and the lowest deviation with reference to the experimental data was obtained for the 6-31G* and 6-311G* basis sets and the B3PW91 functional [6]. In this case the lower difference between theoretical and experimental frequencies, measured by the root mean standard deviation (RMSD) was obtained with the combination B3LYP/6-31+G. We obtained similar results in the study of the $[VOCl_4]^-$ anion [5]. In the study of the structures and vibrational spectra of chromium oxo anions and oxyhalide compounds, Bell and Dines [19] have found that B3LYP/Lanl2DZ combination gives the best fit for the geometries and observed vibrational spectra.

In this case, we used DFT calculations to study the structure and the vibrational properties of the compound. The normal mode calculations were accomplished by use of a GVFF. Here, we demonstrate that a molecular force field for the chromyl nitrate, considering the nitrate group as well as monodentate and bidentate ligand calculated using the DFT/Lanl2DZ, 6-31G* and 6-311+G combinations is well represented. We obtained the force field scaling factors which produce satisfactory agreement between the calculated and experimental vibrational frequencies of chromyl nitrate. DFT normal mode assignments, in terms of the potential energy distribution (P.E.D.), are in general accord with those obtained from the normal coordinate analysis. Also, the nature of the two types of Cr–O and Cr ← O bonds in chromyl nitrate was systematically and quantitatively investigated by the NBO analysis [20–22]. In addition, the topological properties of electronic charge density are analysed employing Bader's Atoms in Molecules theory (AIM) [23].

2. Experimental

The infrared and Raman spectra of chromyl nitrate, $CrO_2(NO_3)_2$, were taken from a previous study where the compound was obtained as reported in Ref. [16] and from our measurements [1].

3. Computational details

All the calculations were made using the GAUSSIAN 03 [24] set of programs running on a PC Pentium III working under Windows operative system. Geometry calculations were performed using standard gradient techniques and the default convergence criteria as implemented in GAUSSIAN. The starting point for the geometry optimisation was modelled with the GAUSSIAN View program [25]. Calculations were made with hybrid density functional methods (DFT). In that last technique, Becke's three-parameter functional and the non-local correlation provided by Lee–Yang–Parr's (B3LYP) [26,27] expressions were used, as implemented in the GAUSSIAN programs. The Lanl2DZ, STO-3G, 3-21G*, 6-31G, 6-31G*, 6-31+G, 6-31+G*, 6-311G, 6-311G*, 6-311+G and 6-311+G* basis sets were used. For the compound we realized the normal mode analysis using Lanl2DZ, 6-31G* and 6-311+G basis sets.

The harmonic force field in Cartesian coordinates for chromyl nitrate which resulted from the calculations were transformed to "natural" internal coordinates [28] by the MOLVIB program [29,30]. The natural coordinates for monodentate and bidentate chromyl nitrate are shown in Tables 1 and 2, respectively, and have been defined as proposed by Fogarasi and Pulay [31]. Also, the analysis as bidentate ligand was performed with the three basis sets considering the nitrate groups as two rings of four members where the deformations and torsion coordinates of these groups have been defined as proposed by Fogarasi and Pulay [31] and are observed in Table 3. The numbering of the atoms for monodentate and bidentate chromyl nitrate is described in Figs. 1 and 2.

The force field was scaled and refined using, the MOLVIB program [29,30], in which the force constants are multiplied by scale factors until reproducing the experimental frequencies as

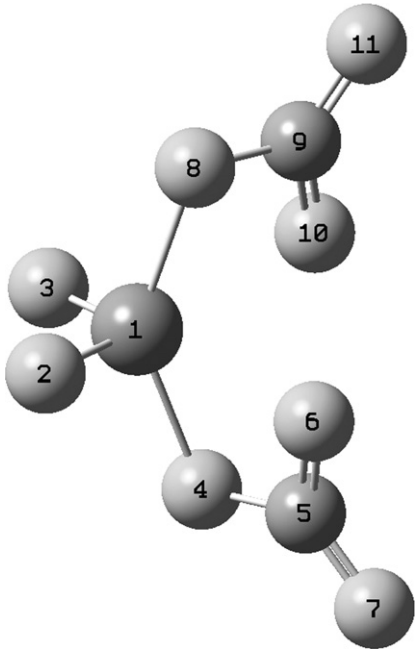

Fig. 1. The molecular structure of chromyl nitrate considering the nitrate group as monodentate ligand.

Table 1
Definition of natural internal coordinates for chromyl nitrate with monodentate coordination adopted by nitrate groups

Symmetry A	
$S_1 = s(5\text{-}7) + s(5\text{-}6) + s(9\text{-}11) + s(9\text{-}10)$	$\nu s(NO_2)$ ip
$S_2 = s(5\text{-}7) + s(9\text{-}11) - s(5\text{-}6) - s(9\text{-}10)$	$\nu a(NO_2)$ ip
$S_3 = q(1\text{-}2) + q(1\text{-}3)$	$\nu s(Cr{=}O)$
$S_4 = 2\beta(6\text{-}5\text{-}7) + 2\beta(10\text{-}9\text{-}11) - \beta(4\text{-}5\text{-}6) - \beta(4\text{-}5\text{-}7) - \beta(8\text{-}9\text{-}10) - \beta(8\text{-}9\text{-}11)$	$\delta(NO_2)$ ip
$S_5 = \gamma(11\text{-}9\text{-}10) - \gamma(7\text{-}5\text{-}4\text{-}6)$	γ N=O op
$S_6 = 2\beta(4\text{-}5\text{-}6) + 2\beta(8\text{-}9\text{-}10) - \beta(4\text{-}5\text{-}7) - \beta(6\text{-}5\text{-}7) - \beta(8\text{-}9\text{-}11) - \beta(10\text{-}9\text{-}11)$	δ(O=N–O) ip
$S_7 = s(5\text{-}4) + s(9\text{-}8)$	νs(N–O)
$S_8 = r(1\text{-}4) - r(1\text{-}8)$	νa(Cr–O)
$S_9 = r(1\text{-}4) + r(1\text{-}8)$	νs(Cr–O)
$S_{10} = \tau(10\text{-}9\text{-}8\text{-}1) + \tau(11\text{-}9\text{-}8\text{-}1) + \tau(7\text{-}5\text{-}4\text{-}1) + \tau(6\text{-}5\text{-}4\text{-}1)$	$\tau(NO_2)$ ip
$S_{11} = \alpha(5\text{-}4\text{-}1) + \alpha(9\text{-}8\text{-}1)$	δ(N–O–Cr) ip
$S_{12} = \tau(3\text{-}1\text{-}4\text{-}5) + \tau(2\text{-}1\text{-}8\text{-}9)$	$\rho(NO_2)$ ip
$S_{13} = \psi(2\text{-}1\text{-}8) + \psi(3\text{-}1\text{-}4) - \psi(2\text{-}1\text{-}4) - \psi(3\text{-}1\text{-}8)$	$\rho(CrO_2)$
$S_{14} = \phi(4\text{-}1\text{-}8)$	δ(O–Cr–O)
Symmetry B	
$S_{15} = s(5\text{-}7) + s(5\text{-}6) - s(9\text{-}11) - s(9\text{-}10)$	$\nu s(NO_2)$ op
$S_{16} = s(5\text{-}7) + s(9\text{-}10) - s(5\text{-}6) - s(9\text{-}11)$	$\nu a(NO_2)$ op
$S_{17} = q(1\text{-}2) - q(1\text{-}3)$	$\nu a(Cr{=}O)$
$S_{18} = 2\beta(6\text{-}5\text{-}7) - 2\beta(10\text{-}9\text{-}11) - \beta(4\text{-}5\text{-}6) - \beta(4\text{-}5\text{-}7) + \beta(8\text{-}9\text{-}10) + \beta(8\text{-}9\text{-}11)$	$\delta(NO_2)$ op
$S_{19} = \gamma(11\text{-}9\text{-}8\text{-}10) + \gamma(7\text{-}5\text{-}4\text{-}6)$	γ N=O ip
$S_{20} = 2\beta(4\text{-}5\text{-}6) - 2\beta(8\text{-}9\text{-}10) + \beta(8\text{-}9\text{-}10) + \beta(10\text{-}9\text{-}11) - \beta(4\text{-}5\text{-}7) - \beta(6\text{-}5\text{-}7)$	δ(O=N–O) op
$S_{21} = s(5\text{-}4) - s(9\text{-}8)$	νa(N–O)
$S_{22} = \theta(2\text{-}1\text{-}3)$	$\delta(CrO_2)$
$S_{23} = \psi(2\text{-}1\text{-}4) + \psi(3\text{-}1\text{-}4) - \psi(2\text{-}1\text{-}8) - \psi(3\text{-}1\text{-}8)$	wag(CrO_2)
$S_{24} = \alpha(5\text{-}4\text{-}1) - \alpha(9\text{-}8\text{-}1)$	δ(N–O–Cr) op
$S_{25} = \tau(3\text{-}1\text{-}4\text{-}5) - \tau(2\text{-}1\text{-}8\text{-}9)$	$\rho(NO_2)$ op
$S_{26} = \tau(10\text{-}9\text{-}8\text{-}1) + \tau(11\text{-}9\text{-}8\text{-}1) - \tau(7\text{-}5\text{-}4\text{-}1) - \tau(6\text{-}5\text{-}4\text{-}1)$	$\tau(NO_2)$ op
$S_{27} = \psi(3\text{-}1\text{-}4) + \psi(3\text{-}1\text{-}8) - \psi(2\text{-}1\text{-}4) - \psi(2\text{-}1\text{-}8)$	τ wis(CrO_2)

q = Cr=O bond distance; r = Cr–O bond distance; s = N–O bond distance; θ = O=Cr=O bond angle; ϕ = O–Cr–O bond angle; ψ = O=Cr–O bond angles; α = Cr–O–N bond angle; β = O–N–O bond angle. Abbreviations: ν, stretching; δ, deformation; ρ, in the plane bending or rocking; γ, out of plane bending or wagging; τw, twisting; a, antisymmetric, s, symmetric; ip, in phase; op, out of phase.

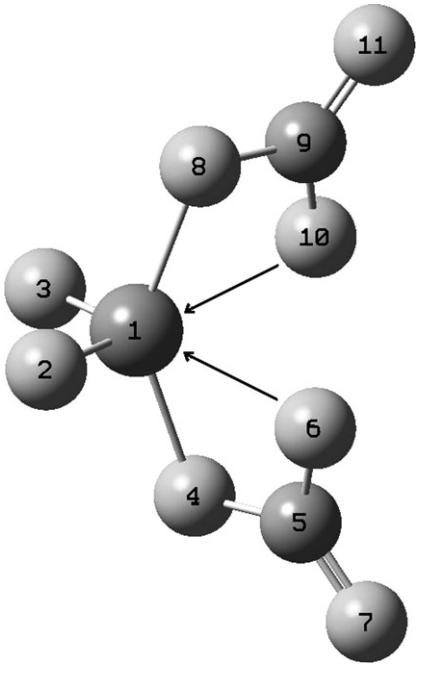

Fig. 2. The molecular structure of chromyl nitrate considering the nitrate group as bidentate ligand.

well as possible. The potential energy distribution components larger than or equal to 10% are subsequently calculated with the resulting scaled quantum mechanics (SQM) force field.

An NBO analysis was then performed using the same basis sets with the NBO 3.1 program [32] included in GAUSSIAN 03 package programs [24]. The topological properties of the charge density in all systems studied were computed with the AIM2000 software [33].

4. Results and discussion

4.1. Geometry calculations

The B3LYP structures obtained for chromyl nitrate with the different basis sets have C_2 symmetries like to the experimental structure obtained by diffraction data and HF method by Marsden et al. [12]. Table 4 shows the comparison of the total energies and dipole moments values for chromyl nitrate with the B3LYP method using different basis sets. In all cases, the more stable structure is obtained using B3LYP/6-311+G* method combined with a diffuse function basis set while the structure with higher energy is obtained by B3LYP/Lanl2DZ calculation. The higher dipole moment value agrees with the one obtained with the 6-311+G* basis set and this indicates that the largest dipole moment value stabilizes the molecule.

Table 2
Definition of natural internal coordinates for chromyl nitrate with bidentate coordination adopted by nitrate groups

Symmetry A	
$S_1 = s(5\text{-}7) + s(9\text{-}11)$	ν(N═O) ip
$S_2 = s(4\text{-}5) + s(9\text{-}10) - s(5\text{-}6) - s(8\text{-}9)$	$\nu a(NO_2)$ op
$S_3 = q(1\text{-}2) + q(1\text{-}3)$	νs(Cr═O)
$S_4 = 2\beta(4\text{-}5\text{-}6) + 2\beta(8\text{-}9\text{-}10) - \beta(4\text{-}5\text{-}7) - \beta(6\text{-}5\text{-}7) - \beta(8\text{-}9\text{-}11) - \beta(10\text{-}9\text{-}11)$	$\delta(NO_2)$ ip
$S_5 = \gamma(11\text{-}9\text{-}8\text{-}10) - \gamma(7\text{-}5\text{-}4\text{-}6\text{-})$	γ N═O op
$S_6 = s(4\text{-}5) + s(5\text{-}6) - s(8\text{-}9) - s(9\text{-}10)$	$\nu s(NO_2)$ op
$S_7 = 2\beta(5\text{-}6\text{-}7) - 2\beta(9\text{-}10\text{-}11) + \beta(8\text{-}9\text{-}10) + \beta(8\text{-}9\text{-}11) - \beta(4\text{-}5\text{-}6) - \beta(4\text{-}5\text{-}7)$	δ(O═N–O) op
$S_8 = \theta(2\text{-}1\text{-}3)$	$\delta(CrO_2)$
$S_9 = r(1\text{-}4) + r(1\text{-}6) + r(1\text{-}8) + r(1\text{-}10)$	νs(Cr–O)
$S_{10} = \psi(2\text{-}1\text{-}6) + \psi(2\text{-}1\text{-}4) + \psi(3\text{-}1\text{-}8) + \psi(3\text{-}1\text{-}10) - \psi(3\text{-}1\text{-}6) - \psi(3\text{-}1\text{-}4) - \psi(2\text{-}1\text{-}8) - \psi(2\text{-}1\text{-}10)$	$\rho(CrO_2)$
$S_{11} = r(1\text{-}4) + r(1\text{-}8) - r(1\text{-}6) - r(1\text{-}10)$	νa(Cr–O)
$S_{12} = \psi(2\text{-}1\text{-}6) + \psi(3\text{-}1\text{-}6) + \psi(2\text{-}1\text{-}8) + \psi(3\text{-}1\text{-}8) - \psi(2\text{-}1\text{-}4) - \psi(3\text{-}1\text{-}4) - \psi(2\text{-}1\text{-}10) - \psi(3\text{-}1\text{-}10)$	$\tau w(CrO_2)$
$S_{13} = r(1\text{-}4) + r(1\text{-}6) - r(1\text{-}8) - r(1\text{-}10)$	νs(Cr ← O)
$S_{14} = \tau(10\text{-}9\text{-}8\text{-}1) + \tau(11\text{-}9\text{-}8\text{-}1) + \tau(7\text{-}5\text{-}4\text{-}1) + \tau(6\text{-}5\text{-}4\text{-}1)$	$\tau(NO_2)$ ip
Symmetry B	
$S_{15} = s(5\text{-}7) + s(9\text{-}11)$	ν(N═O) op
$S_{16} = s(4\text{-}5) + s(8\text{-}9) - s(5\text{-}6) - s(9\text{-}10)$	$\nu a(NO_2)$ ip
$S_{17} = q(1\text{-}2) - q(1\text{-}3)$	νa(Cr═O)
$S_{18} = 2\beta(4\text{-}5\text{-}6) - 2\beta(8\text{-}9\text{-}10) + \beta(8\text{-}9\text{-}10) + \beta(10\text{-}9\text{-}11) - \beta(4\text{-}5\text{-}7) - \beta(6\text{-}5\text{-}7)$	$\delta(NO_2)$ op
$S_{19} = \gamma(11\text{-}9\text{-}8\text{-}10) + \gamma(7\text{-}5\text{-}4\text{-}6)$	γ N═O ip
$S_{20} = s(4\text{-}5) + s(5\text{-}6) + s(8\text{-}9) + s(9\text{-}10)$	$\nu s(NO_2)$ ip
$S_{21} = 2\beta(5\text{-}6\text{-}7) + 2\beta(9\text{-}10\text{-}11) - \beta(4\text{-}5\text{-}6) - \beta(4\text{-}5\text{-}7) - \beta(8\text{-}9\text{-}10) - \beta(8\text{-}9\text{-}11)$	δ(O═N–O) ip
$S_{22} = r(1\text{-}4) + r(1\text{-}6) - r(1\text{-}8) - r(1\text{-}10)$	νa(Cr ← O)
$S_{23} = \tau(10\text{-}9\text{-}8\text{-}1) + \tau(11\text{-}9\text{-}8\text{-}1) - \tau(7\text{-}5\text{-}4\text{-}1) - \tau(6\text{-}5\text{-}4\text{-}1)$	$\tau(NO_2)$ op
$S_{24} = \psi(2\text{-}1\text{-}6) + \psi(3\text{-}1\text{-}4) + \psi(2\text{-}1\text{-}4) + \psi(3\text{-}1\text{-}6) - \psi(2\text{-}1\text{-}8) - \psi(3\text{-}1\text{-}10) - \psi(2\text{-}1\text{-}10) - \psi(3\text{-}1\text{-}8)$	$wag(CrO_2)$
$S_{25} = \phi(8\text{-}1\text{-}4) + \phi(10\text{-}1\text{-}6)$	δs(O–Cr–O)
$S_{26} = \phi(8\text{-}1\text{-}4) - \phi(10\text{-}1\text{-}6)$	δa(O–Cr–O)
$S_{27} = \tau(3\text{-}1\text{-}4\text{-}5) + \tau(3\text{-}1\text{-}10\text{-}9) - \tau(2\text{-}1\text{-}8\text{-}9) - \tau(2\text{-}1\text{-}6\text{-}5)$	τ(N═O)

q = Cr═O bond distance; r = Cr–O bond distance; s = N–O bond distance; θ = O═Cr═O bond angle; ϕ = O–Cr–O bond angle; ψ = O═Cr–O bond angles; β = O–N–O bond angle. Abbreviations: ν, stretching; δ, deformation; ρ, in the plane bending or rocking; γ, out of plane bending or wagging; τw, twisting; a, antisymmetric, s, symmetric; ip, in phase; op, out of phase.

Although the calculated structure with the Lanl2DZ basis set is unstable, the dipole moment value is comparable to the corresponding values obtained with the 6-31G* and 6-31+G basis sets.

The results of the calculations with all basis sets used can be appreciated in Table 5. According to these results, the method and basis set that best reproduces the experimental geometrical parameters for the chromyl nitrate compound is B3LYP/6-31+G* where the mean difference for bond lengths is 0.019 Å, while with B3LYP/6-311G* it is 4.11° for angles. The inclusion of polarization functions, however, is important to have a better agreement with the experimental geometry: mean differences degrade to 0.020 Å and 4.24° for the 6-311+G* basis set. The B3LYP functional gives somewhat less satisfactory agreement using the Lanl2DZ (0.399 Å and 7.90°) and STO-3G (0.107 Å and 5.42) basis sets, contrary to what was observed by Bell and Dines [19] in chromium oxo anions and oxyhalides compounds. In our case, similarly to the experimental structure [12], also with B3LYP calculations, we can represent the coordination around Cr as derived from a severely distorted octahedron where the nitrate groups act as bidentate ligands and are asymmetrically bonded to Cr. The bond orders, expressed by Wiberg's indexes for chromyl nitrate are given in Tables S1 and S2 of the Supporting Material. We can see that the chromium atom forms six bonds, two Cr═O bonds (bond order 1.9721 using 6-311+G basis set), two Cr–O (bond order 0.5374 using 6-311+G basis set) and two Cr ← O (bond order 0.1821 using 6-311+G basis set). The bond order value of this last bond was estimated by Marsden et al. [12] between 0.19 and 0.29. Experimentally the Cr–O–NO_2 group is slightly non-planar with the dihedral angle of the planes Cr–O–N and NO_2 equal to 16° while in our B3LYP calculations the Cr–O–N–O angle values are between 0.9 and 2.0°, as can be seen in Table 5. In this case the two NO_2 groups are practically planar with the Cr atom and there is a slightly torsional motion around either of the Cr–O bonds as was observed by the diffraction method. However, the bond orders obtained for chromyl nitrate with the three basis sets agree with the 0.4 values reported in symmetrically bidentate nitrate groups [7].

Other very important observations in these B3LYP calculations carried out precisely by Marsden et al. [12] with *ab initio* method are those that predict that the O2═Cr1═O3 bond angle in chromyl nitrate is smaller than the O4–Cr1–O8 angle, in contradiction with the valence-shell electron-pair (VSEPR) theory [34,35]. In fact, that theory predicts a larger angle between the bonds of the central atom with the two oxygen atoms in these pseudo-tetrahedral species as a consequence of the larger space in the coordination sphere requested by the pair of double bonds. In this case a possible explanation for the inverse angle relationship is due to the octahedral coordination for the Cr atom in the compound. A possible explanation for the inverse relationship obtained for chromyl nitrate can be given in terms of the

Table 3
Definition of natural internal coordinates for chromyl nitrate with bidentate coordination adopted for nitrate groups (as two rings of four members)

Symmetry A	
$S_1 = s(5\text{-}7) + s(9\text{-}11)$	ν(N═O) ip
$S_2 = s(4\text{-}5) + s(8\text{-}9) - s(5\text{-}6) - s(9\text{-}10)$	$\nu a(NO_2)$ ip
$S_3 = q(1\text{-}2) + q(1\text{-}3)$	νs(Cr═O)
$S_4 = s(4\text{-}5) + s(5\text{-}6) + s(8\text{-}9) + s(9\text{-}10)$	$\nu s(NO_2)$ ip
$S_5 = \beta(6\text{-}5\text{-}4) + \beta(4\text{-}1\text{-}6) + \beta(8\text{-}9\text{-}10) + \beta(10\text{-}1\text{-}8) - \beta(5\text{-}4\text{-}1) - \beta(1\text{-}6\text{-}5) - \beta(9\text{-}10\text{-}1) - \beta(1\text{-}8\text{-}9)$	$\delta(NO_2)$ ip
$S_6 = \gamma(11\text{-}9\text{-}8\text{-}10) + \gamma(7\text{-}5\text{-}4\text{-}6)$	γN═O ip
$S_7 = \beta(4\text{-}5\text{-}7) + \beta(8\text{-}9\text{-}11) - \beta(5\text{-}6\text{-}7) - \beta(10\text{-}9\text{-}11)$	δ(O═N–O) ip
$S_8 = \theta(2\text{-}1\text{-}3)$	$\delta(CrO_2)$
$S_9 = r(1\text{-}4) + r(1\text{-}6) + r(1\text{-}8) + r(1\text{-}10)$	νs(Cr–O)
$S_{10} = \psi(2\text{-}1\text{-}6) + \psi(2\text{-}1\text{-}4) + \psi(3\text{-}1\text{-}8) + \psi(3\text{-}1\text{-}10) - \psi(3\text{-}1\text{-}6) - \psi(3\text{-}1\text{-}4) - \psi(2\text{-}1\text{-}8) - \psi(2\text{-}1\text{-}10)$	$\rho(CrO_2)$
$S_{11} = r(1\text{-}4) + r(1\text{-}8) - r(1\text{-}6) - r(1\text{-}10)$	νa(Cr–O)
$S_{12} = \phi(8\text{-}1\text{-}4) - \phi(10\text{-}1\text{-}6)$	δa(O–Cr–O)
$S_{13} = \tau(6\text{-}1\text{-}4\text{-}5) + \tau(4\text{-}5\text{-}6\text{-}1) + \tau(8\text{-}1\text{-}10\text{-}9) + \tau(10\text{-}9\text{-}8\text{-}1) - \tau(1\text{-}4\text{-}5\text{-}6) + \tau(5\text{-}6\text{-}1\text{-}4) + \tau(1\text{-}10\text{-}9\text{-}8) - \tau(9\text{-}8\text{-}1\text{-}10)$	$\tau(NO_2)$ ip
$S_{14} = \tau(6\text{-}1\text{-}4\text{-}5) + \tau(4\text{-}5\text{-}6\text{-}1) + \tau(1\text{-}10\text{-}9\text{-}8) + \tau(9\text{-}8\text{-}1\text{-}10) - \tau(1\text{-}4\text{-}5\text{-}6) - \tau(5\text{-}6\text{-}1\text{-}4) - \tau(8\text{-}1\text{-}10\text{-}9) - \tau(10\text{-}9\text{-}8\text{-}1)$	$\tau(NO_2)$ op
Symmetry B	
$S_{15} = s(5\text{-}7) - s(9\text{-}11)$	ν(N═O) op
$S_{16} = s(4\text{-}5) + s(9\text{-}10) - s(5\text{-}6) - s(8\text{-}9)$	$\nu a(NO_2)$ op
$S_{17} = q(1\text{-}2) - q(1\text{-}3)$	νa(Cr═O)
$S_{18} = s(4\text{-}5) + s(5\text{-}6) - s(8\text{-}9) - s(9\text{-}10)$	$\nu s(NO_2)$ op
$S_{19} = \beta(6\text{-}5\text{-}4) + \beta(4\text{-}1\text{-}6) + \beta(9\text{-}10\text{-}1) + \beta(1\text{-}8\text{-}9) - \beta(5\text{-}4\text{-}1) - \beta(1\text{-}6\text{-}5) - \beta(8\text{-}9\text{-}10) - \beta(10\text{-}1\text{-}8)$	$\delta(NO_2)$ op
$S_{20} = \gamma(11\text{-}9\text{-}8\text{-}10) - \gamma(7\text{-}8\text{-}4\text{-}6)$	γN═O op
$S_{21} = \beta(4\text{-}5\text{-}7) + \beta(10\text{-}9\text{-}11) - \beta(5\text{-}6\text{-}7) - \beta(8\text{-}9\text{-}11)$	δ(O═N–O) op
$S_{22} = r(1\text{-}4) + r(1\text{-}6) - r(1\text{-}8) - r(1\text{-}10)$	νs(Cr ← O)
$S_{23} = \psi(2\text{-}1\text{-}6) + \psi(3\text{-}1\text{-}4) + \psi(2\text{-}1\text{-}4) + \psi(3\text{-}1\text{-}6) - \psi(2\text{-}1\text{-}8) - \psi(3\text{-}1\text{-}10) - \psi(2\text{-}1\text{-}10) - \psi(3\text{-}1\text{-}8)$	$wag(CrO_2)$
$S_{24} = \psi(2\text{-}1\text{-}6) + \psi(3\text{-}1\text{-}6) + \psi(2\text{-}1\text{-}8) + \psi(3\text{-}1\text{-}8) - \psi(2\text{-}1\text{-}4) - \psi(3\text{-}1\text{-}4) - \psi(2\text{-}1\text{-}10) - \psi(3\text{-}1\text{-}10)$	$\tau w(CrO_2)$
$S_{25} = \tau(2\text{-}1\text{-}4\text{-}5) + \tau(3\text{-}1\text{-}4\text{-}5) + \tau(2\text{-}1\text{-}8\text{-}9) + \tau(3\text{-}1\text{-}8\text{-}9) + \tau(2\text{-}1\text{-}10\text{-}9) + \tau(3\text{-}1\text{-}10\text{-}9) + \tau(2\text{-}1\text{-}4\text{-}5) + \tau(3\text{-}1\text{-}4\text{-}5)$	τ(N═O)
$S_{26} = \phi(8\text{-}1\text{-}4) + \phi(10\text{-}1\text{-}6)$	δs(O–Cr–O)
$S_{27} = r(1\text{-}6) + r(1\text{-}8) - r(1\text{-}4) - r(1\text{-}10)$	νa(Cr ← O)

q = Cr═O bond distance; r = Cr-O bond distance; s = N–O bond distance; θ = O═Cr═O bond angle; ϕ = O–Cr–O bond angle; ψ = O═Cr–O bond angles; β = O–N–O bond angle. Abbreviations: ν, stretching; δ, deformation; ρ, in the plane bending or rocking; γ, out of plane bending or wagging; τw, twisting; a, antisymmetric, s, symmetric; ip, in phase; op, out of phase.

calculated Mulliken atomic charges. Such charges, taken from the DFT calculations (see Table S2 using 6-31G* and 6-311+G basis sets), have the following values: Cr 1.364, O2 −0.317, O3 −0.317 and O4 −0.438, O8 −0.438. These numbers show (using 6-31G* basis set) that the remarkably higher negative charge on the oxygen atoms of chromyl nitrate could result in a relatively larger O···O repulsion and consequently in a larger O4–Cr1–O8 angle (141.6°), which for such compound exceeds the O2–Cr1–O3 angle (107.9°). It is interesting to observe that these values of Mulliken atomic charges are very different from those attained at B3LYP/Lanl2DZ and B3LYP/6-311+G* levels, only as regards the numerical values but not the relative order within them. The inclusion of diffuse functions makes the charge on the oxygen bounded to the Cr atom to be lower (O═Cr═O) than that located on the other O atoms (O–Cr–O) in this case these values are positive as shown in Table S2. This leads to the conclusion that any analysis based on the Mulliken atomic charges must be made with care as it is apparent that a satisfactory explanation based on electronegativity criteria is not affordable [3]. A somewhat different but related explanation might be tried on the basis of the delocalised and/or bonding characters of the relevant molecular orbitals (MO), as observed in the series of the $VO_2X_2^-$ anions [3]. After a careful inspection of the atomic orbital coefficients (AO) appearing in the different MO it is possible to note that as a general pattern, the highest occupied MO's show a rather localised character on the oxygen atoms being mainly described as p-type orbitals. The atomic orbital coefficients (AO) for Cr atom of chromyl nitrate (d-type orbitals) using Lanl2DZ, 6-31G* and 6-311+G basis sets are observed in Table S3 of the Supporting Material. For the chromyl nitrate the strongest bonding MO's involving Cr d-type orbitals that seem to be sensitive to the geometry can be considered, in increasing energy, those numbered as 13 (HOMO-31); 13 (HOMO-36) and 14 (HOMO-32) calculated with Lanl2DZ basis set; 20 (HOMO-36), 21 (HOMO-36) and 22 (HOMO-37) calculated with 6-31G* basis set while those numbered as 25 (HOMO-36), 26 (HOMO-37) and 31 (HOMO-37) calculated

Table 4
Total energy and dipole moment for chromyl nitrate at B3LYP method

Basis set	ET (Hartree)	μ (D)
Lanl2DZ	−797.26788972	0.54
STO-3G	−1735.04954605	0.14
3-21G*	−1746.64837014	0.28
6-31G	−1755.21237919	0.43
6-31G*	−1755.48635040	0.50
6-311G	−1755.49143234	0.67
6-31+G	−1755.25752525	0.59
6-31+G*	−1755.51881813	0.71
6-311G*	−1755.73534229	0.70
6-311+G	−1755.52645780	0.63
6-311+G*	−1755.76567840	0.73

Table 5
Comparison of experimental and calculated geometrical parameters at different levels of theory for chromyl nitrate

Atoms	B3LYP method[a]												
	Lanl2DZ	STO-3G	3-21G	6-31G	6-31+G	6-31+G*	6-31G*	6-311G	6-311G*	6-311+G	6-311+G*	Exp.[b]	*ab initio*[b]
Bond length (Å)													
1,2	1.568	1.484	1.561	1.573	1.577	1.554	1.548	1.569	1.546	1.574	1.550	1.586	1.522
1,3	1.568	1.484	1.561	1.573	1.577	1.554	1.548	1.569	1.546	1.574	1.550	1.586	1.522
1,4	1.914	1.864	1.888	1.933.	1.935	1.923	1.920	1.933	1.916	1.941	1.924	1.957	1.958
1,8	1.914	1.864	1.888	1.933	1.935	1.923	1.920	1.933	1.916	1.941	1.924	1.957	1.958
1,6	1.409	2.155	2.205	2.275	2.287	2.243	2.229	2.283	2.253	2.284	2.263	2.254	2.191
1,10	1.310	2.155	2.205	2.275	2.287	2.243	2.229	2.283	2.253	2.284	2.263	2.254	2.191
4,5	1.231	1.436	1.432	1.397	1.396	1.340	1.340	1.394	1.342	1.393	1.342	1.341	1.342
5,6	1.409	1.372	1.325	1.296	1.296	1.261	1.261	1.298	1.255	1.298	1.254	1.254	1.342
5,7	1.310	1.294	1.222	1.216	1.218	1.195	1.194	1.219	1.185	1.220	1.186	1.193	1.205
8,9	1.231	1.436	1.432	1.397	1.396	1.340	1.340	1.394	1.342	1.393	1.342	1.341	1.342
9,10	1.568	1.372	1.325	1.296	1.296	1.261	1.261	1.298	1.257	1.298	1.254	1.254	1.342
9,11	1.568	1.294	1.222	1.216	1.218	1.195	1.194	1.219	1.185	1.220	1.186	1.193	1.205
RMSD (Å)	0.399	0.107	0.060	0.033	0.034	0.019	0.024	0.034	0.024	0.033	0.020		
Bond angle (°)													
2,1,3	108.2	107.5	107.1	107.8	107.9	108.0	107.9	108.0	108.0	107.9	108.1	112.6	105.0
2,1,4	105.2	103.2	104.6	104.9	105.1	105.5	105.2	104.8	104.8	105.2	105.4	97.2	105.5
2,1,8	97.3	96.2	96.9	97.3	97.3	97.0	97.1	96.9	97.5	97.1	97.5	104.5	105.5
3,1,4	97.3	96.2	96.9	97.3	97.3	97.0	97.1	96.9	97.5	97.1	97.5	104.5	105.5
3,1,8	105.2	103.2	104.6	104.9	105.1	105.5	105.2	104.8	104.8	105.2	105.4	97.2	105.5
4,1,8	141.2	146.9	143.4	141.9	141.6	141.3	141.6	142.6	141.6	141.6	140.6	140.4	146.9
6,1,10	101.0	72.6	73.2	73.5	73.9	75.0	74.5	74.3	74.6	73.8	74.5	82.8	
1,4,5	110.0	96.7	97.9	99.5	99.9	99.6	99.2	99.9	100.1	99.7	100.2	97.5	99.0
4,5,6	121.2	108.2	108.7	110.3	110.5	111.5	111.4	110.3	111.4	110.5	111.6	112.2	
4,5,7	128.7	123.3	122.1	121.3	121.2	120.9	120.9	121.3	120.8	121.3	120.7	119.7	
6,5,7	101.0	128.4	129.2	128.4	128.3	127.6	127.6	128.4	127.8	128.2	127.7	128.1	
1,8,9	110.0	96.7	97.9	99.5	99.9	99.6	99.2	99.9	100.1	99.7	100.2	97.5	99.0
8,9,10	121.2	108.2	108.7	110.3	110.5	111.5	111.4	110.3	111.4	110.5	111.6	112.2	
8,9,11	128.7	123.3	122.1	121.4	121.2	120.9	120.9	121.3	120.8	121.3	120.7	119.7	
10,9,11	108.23	128.4	129.2	128.4	128.3	127.6	127.6	128.4	127.8	128.2	127.7	128.1	
RMSD (°)	7.90	5.42	4.49	4.23	4.27	4.36	5.00	4.33	4.11	4.33	4.24		
Bond dihedral angle (degrees)													
2,1,4,5	−82.6	−84.9	−84.2	−83.8	−83.2	−82.5	−83.0	−83.6	−83.1	−83.5	−82.8		
3,1,4,5	166.2	165.4	166.0	165.4	165.9	166.4	166.1	165.6	165.9	165.6	165.9		
8,1,4,5	40.6	39.4	39.8	39.7	40.2	40.7	40.3	39.9	40.4	39.9	40.4		
2,1,8,9	166.2	165.4	166.0	165.4	165.9	166.4	166.1	165.6	165.9	165.6	165.9		
3,1,8,9	−82.6	−84.9	−84.2	−83.8	−83.2	−82.5	−83.0	−83.6	−83.1	−83.5	−82.8		
4,1,8,9	40.6	39.4	39.8	39.7	40.2	40.7	40.3	39.9	40.4	39.9	40.4		
1,4,5,6	−1.3	−1.957	−1.6	−0.9	−1.3	−1.2	−1.1	−0.8	−1.1	−0.9	−0.9	16	
1,4,5,7	179.1	179.4	178.9	179.6	178.9	179.0	179.2	179.0	179.2	179.4	179.3		
1,8,9,10	−1.3	−195.7	−156.3	−0.9	−1.3	−1.2	−11.2	−0.8	−11.3	−0.9	−0.9		
1,8,9,11	179.1	179.4	178.9	179.6	178.9	179.0	179.2	179.7	179.2	179.4	179.3		

[a] This work.
[b] Ref. [12].

with 6-311+G basis set tend to widen the O4–Cr1–O8 angle (125.3° using 6-31G* basis set) on a maximum overlapping basis.

For chromyl nitrate the intermolecular interactions have been analysed by using Bader's topological analysis of the charge electron density, $\rho(r)$ by means of the AIM program [33]. It is necessary to clarify that in this study, the Lanl2DZ, 6-31G* and 6-311+G basis sets have been considered because there are numerous references where the quality of the basis set has no influence on the topological results [36,37] but, in this case there is a significative difference among them as can be seen in Table S4 of the Supporting Material.

The localisation of the critical points in the $\rho(r)$ and the values of the Laplacian at these points are important for the characterization of molecular electronic structure in terms of interactions nature and magnitude. The details of the molecular models for the compound studied showing the geometry of all their critical points is observed in Fig. 3. The analyses of the Cr ← O bonds critical points in the compound studied are reported with the two basis sets in Table S4. In this case two important observations can be seen for the three basis sets. In one case, the Cr1 ← O6 and Cr1 ← O10 bonds critical points have the typical properties of the closed-shell interaction. That is, the value of $\rho(r)$ are relatively low (0.05 and 0.3 a.u.), the

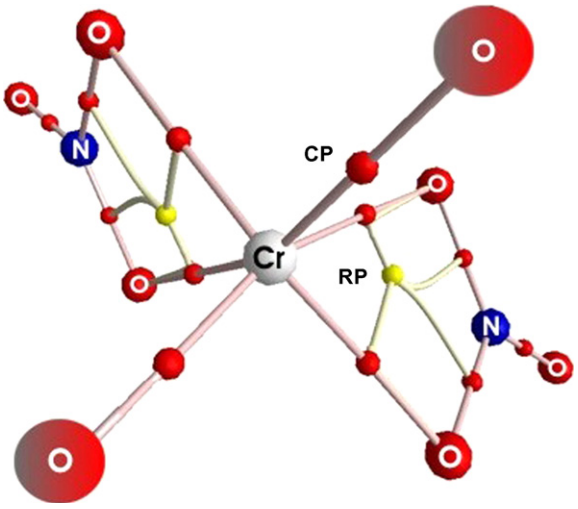

Fig. 3. The critical points of the charge density for chromyl nitrate.

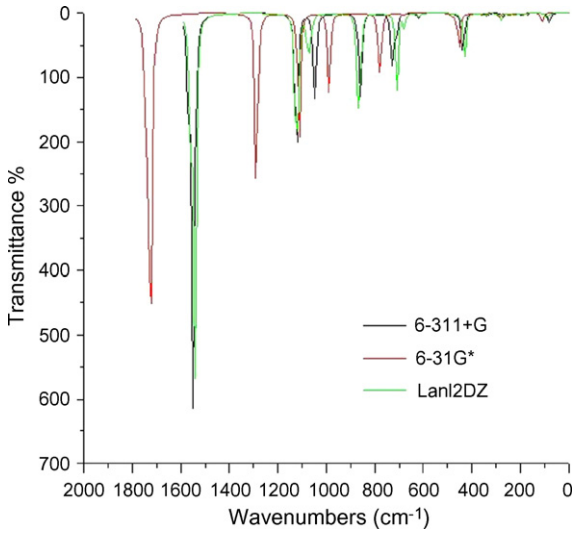

Fig. 4. Theoretical Infrared spectrum of $CrO_2(NO_3)_2$ at different levels of theory.

relationship, $|\lambda 1|/\lambda 3$ are <1 and the Laplacian of the electron density, $\nabla^2\rho(r)$ (0.04 and 0.2 a.u.), are positive indicating that the interaction is dominated by the contraction of charge away from the interatomic surface toward each nucleus [36–43]. The $\rho(r)$ and $\nabla^2\rho(r)$ at the critical points related to Cr1 ← O10 bonds, which compare well with the respective 0.395 and 1.164 a.u. values reported for the Cr–O bond critical point in the $CrOF_4$ compound [35]. The other important observation, is related to the topological properties of the Cr1 ← O6 and Cr1 ← O10 bonds critical points as shown in Table S4. In these cases, the electron densities values are between 0.4 and 0.5 a.u. while the negative values of the Laplacian of the electron density for the Cr ← O bonds (−0.2 and −0.8 a.u.), observed in Table S4, indicate that the Cr1 ← O6 and Cr1 ← O10 bonds critical points are not found in a region of charge depletion. The interaction Cr1 ← O10 bond is the same as the Cr1 ← O6 bond, which has the characteristic of the shared interaction, i.e. the value of electron density at the bond critical point is relatively high and the Laplacian of the charge density is negative indicating that the electronic charge is concentrated in the internuclear region. These values of the Laplacian of the charge density compare well with the −1.096 a.u. values reported for the C–H bond critical point in the VMe_5 compound [35]. Moreover, the (3,+1) critical point as shown in Table S4 in the chromyl nitrate would confirm the two Cr ← O bond in the respective structure. The 12 critical points and the 2 ring points of the electron density obtained by AIM analysis reveals that the mode of coordination adopted for the nitrate groups in chromyl nitrate is bidentate, as shown in Fig. 3. Those above B3LYP level results analysed for chromyl nitrate are in agreement with the structure observed by electron-diffraction experiments in gas phase and strongly support the conclusions reported previously about the nature of the coordination of the Cr atom for this compound [12].

4.2. Vibrational frequencies

The structure for the compound has C_2 symmetry and 27 vibrational normal modes. All vibrational modes are infrared and Raman active. As it is impossible to make a difference between monodentate and bidentate nitrate groups on the grounds of infrared and Raman spectra alone [7,9] we have performed this study taking into account both possibilities. The observed frequencies and the assignment for chromyl nitrate considering the coordination adopted by nitrate groups as monodentate and bidentate are given in Table 6. Vibrational assignments were made on the basis of the potential energy distributions in terms of symmetry coordinates and by comparison with molecules that contain similar groups [1,44–52].

Table S5 of the Supporting Material shows the calculated harmonic frequencies for chromyl nitrate using B3LYP method with different basis sets. Note that the lowest theoretical frequency was not observed in the vibrational spectrum and for this reason we took these frequencies as experimental values. In all cases the theoretical values were compared with the respective experimental values by means of the RMSD values. It can be seen that the best results are obtained with a B3LYP/6-311+G calculation and that the introduction of diffuse functions (but not of polarization functions!) is essential to have a good approximation to the experimental values, especially in the case of the Cr=O and Cr–O stretchings. We will refer to the results obtained at B3LYP level with 6-31G* basis set because after scaling this method a satisfactory agreement is obtained between the calculated and the experimental vibrational frequencies of chromyl nitrate. In general, the theoretical infrared and Raman spectra of the chromyl nitrate demonstrate good agreement with the experimental spectrum (especially in the higher intensity of the Cr=O stretching bands (see Figs. 4 and 5). It is possible to observe that in all calculations some vibration modes of different symmetries are mixed among them because the frequencies are approximately the same.

Bellow we discuss the assignment of the most important groups for the compounds studied considering the two coordination kinds (see Tables 7–9 and Tables S6–S11 of the Supporting Material).

Table 6
Experimental frequencies (cm^{-1}) for chromyl nitrate

Experimental spectra[a]				Assignment[b]			Assignment[a]
IR gas[a]	IR liquid[a]	IR solid[a]	Raman liquid[a]	Monodentate	Bidentate	Bidentate[c]	
1900 vvw	1893 vvw	1910		959 + 945 = 1904			1224 + 685 = 1909
1650 sh	1640 sh	1660 sh	1642 (16)	$\nu_s NO_2$ ip	ν N=O ip	ν N=O ip	ν_a N=O
1637 vs	1613 vs	1635 vs	1614 sh	$\nu_s NO_2$ op	ν N=O op	ν N=O op	
1556	1550 w	1550					2 × 778 = 1556
		1381					944 + 453 = 1397
		1348					1223 + 125 = 1348
		1337		1234 + 100 = 1334			
	1305 w						958 + 349 = 1307
	1275	1276		1637 − 349 = 1288			
1227	1234 sh		1232 (11)	$\nu_a NO_2$ ip	$\nu_a NO_2$ ip	$\nu_a NO_2$ ip	ν_s N=O
1221	1215 s	1223	1216 sh	$\nu_a NO_2$ op	$\nu_a NO_2$ op	$\nu_a NO_2$ op	
		1023					775 + 247 = 1022
961		968		835 + 125 = 960			ν_a Cr=O
	958 s	962 sh	959 (100)	ν_s Cr=O	ν_s Cr=O	ν_s Cr=O	ν_s Cr=O
		944	945 sh	ν_a Cr=O	ν_a Cr=O	ν_a Cr=O	ν N–O
		835		δNO_2 ip	δNO_2 ip	$\nu_s NO_2$ ip	γN=O
808 sh	806 sh	800		δNO_2 op	δNO_2 op	$\nu_s NO_2$ op	457 + 349 = 806
781 sh	779 sh	781	782 (8)	γN=O op, γN=Oip	γN=O op, γN=O ip	δNO_2 ip, δNO_2 op	δNO_2
776	771 m	774	774 sh	δO=N–O op, δO=N–O ip	$\nu_s NO_2$ ip, $\nu_s NO_2$ op	γN=Oip, γN=O op	δNO_2
	685 w	689	686 (10)	ν_a N–O, ν_s N–O	δO=N–O op, δO=N–O ip	δO=N–O op, δO=N–O ip	ρNO_2
	457 m	453	460 sh	ν_a Cr–O	δCrO_2	δCrO_2	ν_a Cr–O
			446 (95)	δCrO_2	ν_a Cr–O	ν_s Cr ← O	ν_s Cr–O
	349 w		350 (41)	ν_s Cr–O	ν_s Cr–O	ν_s Cr–O	δCrO_2
	273 w		271 (9)	Wag CrO_2	τNO_2 op	Wag CrO_2	ρ CrO_2
	247 w		242 (5)	τNO_2 ip	ρ CrO_2	ρ CrO_2	δN–O–Cr
	223 sh			δN–O–Cr op	Wag CrO_2	τw CrO_2	
	213 w						
			206 (9)	δN–O–Cr ip, ρNO_2 ip	ν_a Cr ← O δs O–Cr–O	ν_a Cr–O_2, τN=O	
			152 (5)	ρ CrO_2, δO–Cr–O	δa O–Cr–O, τw CrO_2	δaO–Cr–O, δsO–Cr–O	τNO_2
	125 br, vw		100	τNO_2 op, τw CrO_2, δN–O–Cr op, ρNO_2 op	τN=O, ν_s Cr ← O	τNO_2 ip, ν_a Cr ← O	
	–		–		τNO_2 ip	τNO_2 op	

Abbreviations: ν, stretching; δ, deformation; ρ, rocking; wag, (γ) wagging; τw, torsion, a, antisymmetric, s, symmetric op, out of phase; ip, in phase
[a] Ref. [1].
[b] This work.
[c] Considering the nitrate group as ring of four members.

4.2.1. Coordination monodentate of the nitrate groups

The infrared and Raman frequencies, their respective intensities and the potential energy distribution obtained by DFT/B3LYP/6-31G*, B3LYP/Lanl2DZ and B3LYP/6-311+G calculations considering monodentate coordination of the nitrate groups appear in Tables 7, S6 and S7, respectively. In all cases the theoretical values were compared with the experimental values by means of the RMSD values. The calculated harmonic force field for chromyl nitrate can be obtained upon request. The frequencies calculated using the 6-311+G basis set for the compound are lower than those obtained using the Lanl2DZ and 6-31G* basis sets. The RMSD initial value using B3LYP/Lanl2DZ and B3LYP/6-31G* calculations are 62.2 and 73.5 cm^{-1} while with the 6-311+G basis set is 53.1 cm^{-1}. It can be seen that the best results for chromyl nitrate are obtained using B3LYP/6-31G* calculation with a RMSD final equal at 19.8 cm^{-1} although the introduction of the polarization function does not have a good approximation to the experimental values. In this case the covalent bonding of the nitrate group is easily recognized from its infrared spectrum because the symmetry group changes from the point group D_{3h} of the free ion to C_{2v} of the compound [7].

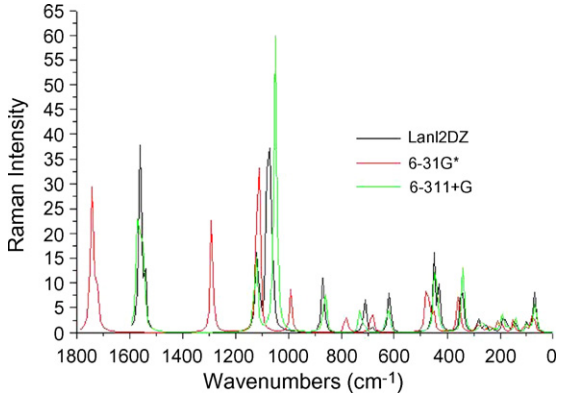

Fig. 5. Theoretical Raman spectrum of $CrO_2(NO_3)_2$ at different levels of theory.

4.2.1.1. Nitrate groups. The strong bands observed in the infrared spectrum reported in previous paper [1] of $CrO_2(NO_3)_2$

Table 7
Experimental and calculated frequencies (cm^{-1}), potential energy distribution and assignment for monodentate chromyl nitrate

Mode	Observed[a]	Calculated[b]	SQM[c]	IR int.[d]	Raman act.[e]	P.E.D. (≥10%)
Symmetry A						
1	1642	1743	1631	227.9	37.2	$65\ S_1 + 14\ S_2 + 10\ S_6$
2	1232	1289	1237	151.3	20.9	$58\ S_2 + 23\ S_1$
3	959	1115	952	93.6	33.1	$94\ S_3$
4	835	991	846	96.5	8.3	$45\ S_4 + 36\ S_{21}$
5	781	785	782	37.2	2.5	$77\ S_5 + 15\ S_{12}$
6	774	778	765	1.8	0.5	$52\ S_6 + 17\ S_9 + 15\ S_{11}$
7	686	684	632	0.3	4.8	$50\ S_7 + 21\ S_{18} + 11\ S_9$
8	460	475	464	4.1	14.6	$71\ S_8 + 11\ S_4$
9	349	356	359	4.9	11.4	$40\ S_{22} + 39\ S_9 + 12\ S_{12}$
10	242	274	262	0.0	1.4	$44\ S_{10} + 17\ S_{13} + 14\ S_{12} + 10\ S_{14}$
11	206	236	223	2.2	1.4	$50\ S_{11} + 12\ S_{12} + 10\ S_9$
12	206	207	192	0.6	2.7	$55\ S_{12} + 21\ S_{13} + 15\ S_{11}$
13	152	149	137	0.0	2.4	$35\ S_{13} + 29\ S_{10} + 19\ S_{14} + 10\ S_{12}$
14	76	76	75	0.2	5.7	$48\ S_{10} + 40\ S_{12} + 11\ S_{14}$
Symmetry B						
15	1614	1724	1622	815.7	14.6	$67\ S_{15} + 14\ S_{16}$
16	1216	1285	1226	187.9	3.7	$59\ S_{16} + 22\ S_{15}$
17	945	1111	951	155.5	18.8	$91\ S_{17}$
18	800	986	840	45.6	1.0	$47\ S_{18} + 37\ S_7$
19	781	783	781	13.3	0.4	$91\ S_{19}$
20	774	777	762	88.0	1.5	$52\ S_{20} + 17\ S_8 + 15\ S_4 + 11\ S_{27}$
21	686	684	627	4.2	0.9	$56\ S_{21} + 18\ S_{47} + 11\ S_8$
22	446	453	450	78.0	5.7	$63\ S_{22} + 16\ S_{12}$
23	273	287	265	7.8	1.9	$41\ S_{23} + 26\ S_{27} + 22\ S_{26}$
24	223	247	237	3.8	0.4	$45\ S_{24} + 29\ S_{23}$
25	152	191	166	2.9	1.3	$21\ S_{25} + 21\ S_{27} + 17\ S_{23} + 17\ S_{26} + 13\ S_{24}$
26	100	112	100	12.6	0.3	$60\ S_{26} + 35\ S_{27}$
27	100	105	89	1.1	1.6	$27\ S_{25} + 26\ S_{27}$
RMSD (cm^{-1})		73.5	19.8			

[a] This work.
[b] DFT B3LYP/6-31G*.
[c] From scaled quantum mechanics force field.
[d] Units are km mol^{-1}.
[e] Raman activities in $Å^4$ $(amu)^{-1}$.

liquid at 1613 and 1215 cm^{-1}, were assigned to N=O antisymmetric and symmetric stretchings, respectively. In this work, the N=O in phase and out of phase symmetric stretching modes are calculated by the B3LYP/6-31G* method at 1743 and 1724 cm^{-1}, respectively. The B3LYP/Lanl2DZ and B3LYP/6-311+G methods underestimate the N=O stretching frequencies as compared to the experimental values. The frequencies predicted for these vibrational modes show that the two symmetric stretching modes are split by about 19 cm^{-1} with the 6-31G* basis set (using Lanl2DZ and 6-311+G basis sets the splitting is 18 cm^{-1}). These modes are calculated slightly coupled with antisymmetric stretching modes but they are only mixed with the O=N–O in phase deformation mode using 6-31G* and 6-311+G basis sets. Normally, the N=O stretching frequencies of the nitrate ion and nitrate group are observed between 1531 and 1481 cm^{-1} [44,49,50] while in nitrogen oxides they are observed at 1758 and 1660 cm^{-1} [9]. In $[Zr(NO_3)_6]^{2-}$ complex [45] the N=O stretching is observed at 1570 cm^{-1}, in $[Cr(NH_3)_5(ONO)]Cl_2$ complex at 1460 cm^{-1} [49] while this vibration mode in HNO_3 [45] is observed at 1672 cm^{-1}. In the $UO_2(NO_3)_2$ and $Cu(NO_3)_2$ anhydrous salts, the N=O stretching frequencies are observed at 1560 and 1585 cm^{-1} [47,48]. For these observations, the shoulder at 1640 cm^{-1} in the liquid spectrum and the very strong band at 1613 cm^{-1}, with a difference among them of 27 cm^{-1} are assigned to these modes.

The NO_2 in phase and out of phase antisymmetric modes are calculated with B3LYP/6-31G* method at 1289 and 1285 cm^{-1}, respectively. In the three calculations these modes appear coupled with the stretching modes. Generally, in nitro complexes the NO_2 antisymmetric stretching modes are observed between 1488 and 1343 cm^{-1} and in nitrate ion is observed at 1388 cm^{-1} [9,49] while the symmetric mode is observed between 1364 and 1315 cm^{-1} [49]. In the $UO_2(NO_3)_2$ and $Cu(NO_3)_2$ anhydrous salts the NO_2 stretching antisymmetric modes are observed in the 1300 cm^{-1} region while the NO_2 stretching symmetric modes appear approximately at 1000 cm^{-1} [47,48]. In our previous paper [1] only the shoulder in the Raman spectrum at 945 cm^{-1} is assigned to one of these modes. Now, the shoulder in the infrared spectrum of the liquid phase at 1234 cm^{-1} and the strong band in the same spectrum at 1215 cm^{-1} are assigned to NO_2 in phase and out of phase antisymmetric stretching modes, respectively.

Table 8
Experimental and calculated frequencies (cm^{-1}), potential energy distribution and assignment for bidentate chromyl nitrate

Mode	Observed[a]	Calculated[b]	SQM[c]	IR int.[d]	Raman act.[e]	P.E.D. (≥10%)
Symmetry A						
1	1642	1743	1639	227.9	37.2	71 S_1 + 17 S_4
2	1216	1285	1228	151.3	20.9	67 S_2 + 27 S_7
3	959	1115	954	93.6	33.1	95 S_3
4	835	991	829	96.5	8.3	39 S_4 + 28 S_{20} + 10 S_{21}
5	781	785	781	37.2	2.5	61 S_5 + 30 S_{27}
6	774	778	775	1.8	0.5	30 S_{18} + 19 S_5 + 10 S_6
7	686	684	664	0.3	4.8	32 S_7 + 31 S_2 + 24 S_{20}
8	460	475	459	4.1	14.6	72 S_8 + 17 S_9
9	349	356	345	4.9	11.4	40 S_9 + 25 S_8 + 13 S_{11}
10	242	274	262	0.0	1.4	34 S_{10} + 28 S_{25} + 19 S_{14} + 12 S_{11}
11	206	236	222	2.2	1.4	44 S_{11} + 30 S_9 + 14 S_{26}
12	152	191	155	2.9	1.3	40 S_{22} + 31 S_{27} + 11 S_{12}
13	100	112	101	12.6	0.3	26 S_{13} + 24 S_{12} + 20 S_{23}
14	76	76	74	0.2	5.7	54 S_{14} + 41 S_{25}
Symmetry B						
15	1614	1724	1622	815.7	14.6	72 S_{15} + 17 S_{18}
16	1232	1289	1221	187.9	3.7	66 S_2 + 28 S_{21}
17	945	1111	950	155.5	18.8	95 S_{17}
18	800	986	821	45.6	1.0	40 S_{18} + 37 S_6
19	781	783	780	13.3	0.4	83 S_{19}
20	774	777	770	88.0	1.5	38 S_4 + 26 S_{20} + 13 S_9
21	686	684	660	4.2	0.9	33 S_{16} + 28 S_{21} + 27 S_6
22	446	453	428	78.0	5.7	35 S_{24} + 25 S_{22} + 12 S_{27}
23	273	287	274	7.8	1.9	41 S_{23} + 35 S_{24} + 13 S_{12}
24	223	247	227	3.8	0.4	42 S_{24} + 23 S_{12} + 11 S_{22} + 10 S_{13}
25	206	207	198	0.6	2.7	30 S_{11} + 22 S_{26} + 18 S_9 + 14 S_{25}
26	152	149	141	0.0	2.4	46 S_{10} + 30 S_{26} + 12 S_{14}
27	100	105	98	1.1	1.6	52 S_{27} + 33 S_{23}
RMSD (cm^{-1})		73.5	10.6			

[a] This work.
[b] DFT B3LYP/6-31G*.
[c] From scaled quantum mechanics force field.
[d] Units are km mol^{-1}.
[e] Raman activities in $Å^4$ $(amu)^{-1}$.

The NO_2 out of phase and in phase deformation modes are perfectly characterized by the three calculations and are observed coupled with N–O vibration modes. The bands observed in the infrared spectrum at low temperature at 835 and 800 cm^{-1} are assigned to NO_2 in phase and out of phase deformation, respectively. These bands are predicted in the Raman spectrum with all basis sets with low intensity and experimentally are not observed.

Others modes well characterized by the three calculations are the N=O out of plane in phase and out of phase deformation. The P.E.D. values indicate that the O=N–O in phase and out of phase deformation modes are strongly coupled with vibrations of the CrO_2 and NO_2 groups. In nitro complexes these modes are observed among 657 and 433 cm^{-1} [49] while in nitrate ion is observed at 831 cm^{-1} [9,49]. In this case, the band in the IR low temperature at 781 cm^{-1} is assigned to these vibration modes. The band in the IR low temperature observed at 774 cm^{-1} in the previous paper is assigned to these vibration modes [1]. In this case the calculations confirm such assignment.

The N–O antisymmetric and symmetric stretching modes are calculated also coupled with vibrations of nitrate groups as shown in Tables 6–8. In nitrate ion, these modes are observed at 831 cm^{-1} [9,49] while in $UO_2(NO_3)_2$ they appear at 800 cm^{-1} [47]. The weak band in the Raman spectrum at 686 cm^{-1}, previously assigned to nitrate rocking mode [1], is assigned in this case to these vibration modes.

In the region of lower frequencies the vibration modes normally expected for the nitrate groups are the N–O–Cr bending, rocking, wagging and twisting modes as observed in covalent nitrates [45]. All modes, as shown in Tables 7, S6 and S7, appear coupled among them and with other modes of the chromyl group while the P.E.D. values are different in the calculations with all the basis sets.

Experimentally, in the nitro complexes the NO_2 rocking and twisting modes are observed in the low frequencies region between 600 and 400 cm^{-1} and 300 and 240 cm^{-1}, respectively [46,49,50]. In a previous paper we assigned the NO_2 rocking mode at 686 cm^{-1}, the NO_2 torsion at 152 cm^{-1} while the CrO_2 twisting mode was not assigned [1]. In chromyl nitrate the NO_2 in phase and out of phase torsion modes are calculated using the three basis sets which appear strongly mixed and with different P.E.D. Previously, we assigned only one of these modes

Table 9
Experimental and calculated frequencies (cm^{-1}), potential energy distribution and assignment for bidentate coordination adopted for nitrate groups (as two rings of four members)

Mode	Observed[a]	Calculated[b]	SQM[c]	IR int.[d]	Raman act.[e]	P.E.D. (≥10%)
Symmetry A						
1	1642	1743	1638	227.9	37.2	80 S_1 + 11 S_4
2	1232	1289	1182	151.3	20.9	57 S_2 + 29S_7
3	959	1115	955	93.6	33.1	95 S_3
4	835	991	872	96.5	8.3	64 S_4 + 23 S_7 + 11 S_2
5	781	785	789	37.2	2.5	64 S_5 + 22 S_9
6	774	778	776	1.8	0.5	47 S_6 + 33 S_{20}
7	686	684	653	0.3	4.8	42 S_2 + 27 S_7 + 18 S_4
8	460	475	455	4.1	14.6	67 S_8 + 19 S_9
9	349	356	350	4.9	11.4	32 S_8 + 29 S_9 + 14 S_5 + 12 S_{25}
10	242	274	260	0.0	1.4	39 S_{10} + 19 S_{26} + 19 S_{14}
11	206	236	223	2.2	1.4	50 S_{11} + 30 S_9
12	152	191	172	2.9	1.3	23 S_{27} + 22 S_{23} + 14 S_{16} + 12 S_{12} + 12 S_{24}
13	100	112	97	12.6	0.3	50 S_{13} + 24 S_{25} + 20 S_{12}
14	76	76	70	0.2	5.7	48 S_{14} + 26 S_{25} + 25 S_{26}
Symmetry B						
15	1614	1724	1620	815.7	14.6	81 S_{15} + 10 S_{18}
16	1216	1285	1180	187.9	3.7	56 S_{16} + 29 S_{21}
17	945	1111	952	155.5	18.8	92 S_{17}
18	800	986	870	45.6	1.0	61 S_{18} + 25 S_{21} + 10 S_{16}
19	781	783	786	13.3	0.4	65 S_{19} + 20 S_{22}
20	774	777	773	88.0	1.5	47 S_{20} + 31 S_6
21	686	684	646	4.2	0.9	45 S_{16} + 23 S_{21} + 20 S_{18}
22	446	453	444	78.0	5.7	33 S_{22} + 17 S_{19} + 14 S_{23} + 13 S_{21} + 13 S_{27}
23	273	287	276	7.8	1.9	58 S_{23} + 12 S_{13} + 12 S_{12}
24	223	247	235	3.8	0.4	37 S_{24} + 20 S_{27} + 19 S_{22} + 12 S_{23}
25	206	207	193	0.6	2.7	48 S_{25} + 25 S_{11} + 13 S_9
26	152	149	139	0.0	2.4	42 S_{10} + 31 S_{26} + 16 S_{14}
27	100	105	77	1.1	1.6	38 S_{27} + 24 S_{24} + 18 S_{22} + 10 S_{16}
RMSD (cm^{-1})		73.5	23.6			

[a] This work.
[b] DFT B3LYP/6-31G*.
[c] From scaled quantum mechanics force field.
[d] Units are km mol^{-1}.
[e] Raman activities in $Å^4$ $(amu)^{-1}$.

at 152 cm^{-1} [1]. In this work, with the aid of the calculations the very weak band in the Raman spectrum at 242 cm^{-1} is assigned to NO_2 in phase torsion mode while the band in the same spectrum at 100 cm^{-1} is assigned to NO_2 out of phase torsion mode.

The assignment of the N–O–Cr in phase and out of phase bending modes is very difficult because these modes are calculated by three methods used at different frequencies and P.E.D. values. With the B3LYP/6-31G* calculation these modes appear more defined than with the other methods hence the shoulder observed in the IR spectrum of the liquid compound at 223 cm^{-1} and the weak Raman band at 206 cm^{-1} are assigned to N–O–Cr out of phase and in phase modes bending modes, respectively. In our assignment previously realized for this molecule only one of these modes was assigned at 247 cm^{-1} [1].

The NO_2 in phase rocking mode is calculated clearly at 207 cm^{-1} with the B3LYP/6-31G* calculation and with higher P.E.D. value (55%) than with the B3LYP/6-311+G calculation (42%) but, in this last case it is calculated at 201 cm^{-1}. The NO_2 out of phase rocking mode appears mixed, in the three methods used, with different modes such as NO_2 torsion and CrO_2 twisting. This mode, with the B3LYP/6-31G* method is calculated clearly at 112 cm^{-1} coupled with higher P.E.D. value (27%) with the CrO_2 twisting mode while with the B3LYP/6-311+G method it is calculated at 81 cm^{-1} with higher contribution (27%) and, it is also calculated at 173 cm^{-1} but, with lower contribution (21%). Experimentally, in nitro complexes the NO_2 rocking mode is observed in the low frequencies region, between 600 and 400 cm^{-1} [49]. In a previous paper we assigned the NO_2 rocking mode at 686 cm^{-1} [1]. In this case the theoretical calculations show clearly the NO_2 in phase rocking mode and, for this reason the band at 206 cm^{-1} is also assigned to this vibration mode and to the N–O–Cr in phase bending mode. The band in the Raman spectrum at 100 cm^{-1} is assigned to the NO_2 out of phase rocking mode.

4.2.1.2. Chromyl group. The frequencies predicted for the vibrational modes of chromyl nitrate show that the antisymmetric and symmetric Cr=O stretchings are split by more than 4 cm^{-1}, indicating a little contribution of the central Cr atom in these vibrations. The antisymmetric and symmetric Cr=O stretchings modes were observed in the spectrum of the solid

sample at 968 and 962 cm^{-1}, respectively, while the more intense band at 959 cm^{-1} in the Raman spectrum is assigned to the symmetric Cr=O stretching. Tables 7, S6 and S7 for chromyl nitrate show that the unscaled DFT frequencies for the symmetric Cr=O stretchings mode, are higher than the frequencies of the antisymmetric Cr=O stretchings, an observation also reported by us [1]. In this compound these modes are uncoupled with other modes. In other chromyl compounds these modes appear in 1050–900 cm^{-1} region, i.e. in $CrO_2(ClO_4)_2$ they appear at 990 and 980 cm^{-1} [51], in $CrO_2(SO_3F)_2$ appear at 1061 and 1020 cm^{-1} [15] and in CrO_2F_2 and CrO_2Cl_2 they are observed for the first compound at 1016 and 1006 cm^{-1} while for the second one at 1002 and 995 cm^{-1}, respectively [45,49]. In this case the intense band in the Raman spectrum at 959 cm^{-1} is assigned to Cr=O symmetric stretching mode while the shoulder observed in the same spectrum at 945 cm^{-1} is assigned to the corresponding antisymmetric stretching.

Also, the antisymmetric and symmetric Cr–O stretchings are split by more than 26 cm^{-1}, indicating a slight contribution of the central Cr atom in these vibrations. These stretchings in $CrO_2(ClO_4)_2$ they are observed, respectively, at 380 and 355 cm^{-1} [51] and in $CrO_2(NO_3)_2$ were assigned previously by us at 460 and 446 cm^{-1}, respectively [1]. In this case the theoretical calculation predicts these modes with greater P.E.D. value for the antisymmetric mode in reference to the symmetric mode. The intensities of these bands using all basis sets are not predicted correctly because the more intense band is related to the antisymmetric mode. Here, we confirm the assignment previously carried out by us for the antisymmetric mode at 460 cm^{-1}[1] while the band at 350 cm^{-1} of the higher intensity in the Raman spectrum is assigned to Cr–O symmetric stretchings mode.

The CrO_2 bending mode is observed in CrO_2F_2 at 364 cm^{-1} while in CrO_2Cl_2 it is at 356 cm^{-1} [45,49]. The band observed in the Raman spectrum at 350 cm^{-1} is assigned to the CrO_2 bending (O=Cr=O) of chromyl nitrate [1] while the other CrO_2 bending (O–Cr–O) was not assigned. In this work, the B3LYP/6-31G* method calculates the CrO_2 bending at 453 cm^{-1} with 63% of contribution P.E.D. and at 437 cm^{-1} with 56% of contribution P.E.D. With the other basis set this mode appears also coupled. In this case we assigned the intense band in the Raman spectrum at 446 cm^{-1} to CrO_2 bending. The other O–Cr–O bending mode is calculated (at 149 cm^{-1} with 6-31G* basis set and at 141 cm^{-1} with 6-311+G basis set) strongly coupled with other modes. The very weak band observed in the Raman spectrum at 152 cm^{-1} is assigned to O–Cr–O bending. Previously this mode was not assigned by us [1].

The wagging, rocking and twisting modes of the CrO_2 group are not assigned in a previous paper [1]. In this case the calculations predict these modes in the low frequencies region and it is coupled with other modes of the nitrate groups. The wagging CrO_2 mode is calculated using all basis sets at higher frequency and with lower contribution of the P.E.D. than the rocking mode. For these observations, the weak band in the spectrum of the liquid at 273 cm^{-1} is assigned to the wagging mode while the Raman band at 152 cm^{-1} is assigned to the rocking mode.

The CrO_2 twisting mode was not assigned previously. The P.E.D. values indicate that this mode is strongly coupled with vibrations of the same group and the NO_2 group as shown in Tables 7, S6 and S7. It is noticeable how the contribution of the P.E.D. value changes with the method used and it is possible to observe with all basis sets that this mode is strongly mixed at different frequencies (between 273 and 100 cm^{-1}). In this case this mode could be assigned at 100 cm^{-1} because it appears with a higher P.E.D. value.

4.2.2. Coordination bidentate of the nitrate groups

4.2.2.1. Group nitrate without ring. The frequencies, infrared and Raman intensities and potential energy distribution obtained by B3LYP/6-31G*, B3LYP/Lanl2DZ and B3LYP/6-311+G calculations considering the mode of coordination adopted by nitrate groups as bidentate appear in Tables 8, S8 and S9. In the three cases the comparison of the theoretical values with the respective experimental values (RMSD) is observed in the respective tables. The calculated harmonic force field for chromyl nitrate can be obtained upon request. It can be seen that the best results for bidentate coordination of chromyl nitrate are newly obtained with B3LYP/6-31G* calculation with a final RMSD of 10.6 cm^{-1} while with the Lanl2DZ and 6-311+G basis sets the final RMSD were 18.7 and 16.5 cm^{-1}, respectively.

4.2.2.1.1. Nitrate group. The theoretical results show slight changes in the P.E.D. values and in the coupling of the modes. In this case using the two basis sets the N=O stretchings in phase mode appear coupled with the NO_2 deformation in phase mode and, on the other hand, the corresponding out of phase modes are also coupled among them. This way, the shoulder in the spectrum of liquid phase at 1640 cm^{-1} and the very strong band in the same spectrum at 1613 cm^{-1} are assigned to these modes. Both bands in the Raman spectrum are observed at 1642 and 1614 cm^{-1}.

The NO_2 antisymmetric out of phase and in phase frequencies also appear coupled with the corresponding O=N–O out of phase and in phase deformation modes, respectively, but with greater contribution (in the two modes) when the 6-31G* basis set is used. The assignment of these bands is similar to the monodentate type, where the shoulder at 1234 cm^{-1} and the strong band at 1215 cm^{-1} in the infrared spectrum of the liquid phase are assigned to NO_2 antisymmetric in phase and out of phase modes, respectively.

The NO_2 in phase and out of phase deformation modes are also coupled with vibrations of the nitrate groups as shown in Tables 8, S8 and S9. In this case the NO_2 in phase mode is calculated with 6-31G* basis set at 991 cm^{-1} and the corresponding out of phase mode at 986 cm^{-1} while with 6-311+G basis set they are calculated strongly coupled and with a higher contribution of P.E.D. at 863 and 858 cm^{-1}, respectively. The bands in the IR low temperature spectrum are observed at 835 and 800 cm^{-1} are assigned to these vibration modes.

The two N=O out of plane deformation modes (out of phase and in phase) appear strongly coupled when the 6-311+G basis set is used (at 728 and 727 cm^{-1}, respectively). The N=O in phase deformation mode appears uncoupled (6-31G* basis set) at 783 cm^{-1} and with a percentage of 83% in the P.E.D. values while the corresponding out of phase deformation mode is calculated at 785 cm^{-1} (with 61% P.E.D.) slightly coupled with the

N=O torsion mode. In both cases the scaled frequencies are 781 and 780 cm^{-1}, respectively, with 6-31G* basis set and 783 and 777, respectively, with 6-311+G basis. Hence the band in the IR low temperature at 781 and at 782 cm^{-1} in the Raman spectrum is assigned to these vibration modes like in the monodentate type. The two calculations confirm such an assignment.

An important observation in this case is the great difference in frequency that appears between the corresponding NO_2 symmetric out of phase and in phase modes. Particularly, the out of phase mode is strongly coupled with the NO_2 out of phase deformation mode and has lower contribution but, only for the B3LYP/6-31G* calculation. For this last basis set the calculated frequencies are 785 and 777 cm^{-1}, respectively. On the contrary, the NO_2 symmetric out of phase and in phase modes are calculated with 6-311+G basis set with higher percentage P.E.D. than the other basis set and both modes are calculated at the same frequency (714 cm^{-1}). The shoulder in the Raman spectrum of the liquid phase at 774 cm^{-1} is assigned to these vibration modes.

The O=N-O out of phase and in phase deformation modes are also coupled and they are calculated at 618 and 617 cm^{-1} with Lanl2DZ basis set while they appear at 624 and 621 cm^{-1}, with 6-31G* and 6-311+G basis sets, respectively. For this observation, the weak band in the Raman spectrum at 686 cm^{-1} is assigned to these vibration modes. In the monodentate type these modes are assigned at 774 cm^{-1}.

In the low frequencies region the vibration modes of the nitrate group appear strongly coupled with other modes of the chromyl group as shown in Tables 8, S8 and S9. When the nitrate groups present bidentate coordination other vibration modes, besides the N=O torsion mode, as NO_2 out of phase and in phase torsion modes are observed in this region.

The two calculations characterize perfectly the NO_2 in phase torsion mode with a 54% of contribution P.E.D. (6-31G* basis set). The corresponding out of phase mode is observed very mixed with different vibration modes but, the higher contribution to P.E.D. is at 287 cm^{-1} (6-31G* basis set). Both torsion modes are observed coupled with the vibration modes of the chromyl group at 76 and 273 cm^{-1}, respectively. Similarly for the monodentate type, the very weak band in the Raman spectrum at 271 cm^{-1} is assigned to the NO_2 torsion out of phase mode while the NO_2 torsion in phase mode could not be assigned because the lower frequency is not observed in the vibrational spectra for the compound or probably is overlapped with the other bands.

The N=O torsion mode is calculated with higher contribution at 105 cm^{-1} (6-31G* basis set) and 81 cm^{-1} when the size basis set increases. Thus, the observation of a weak band in the Raman spectrum of the liquid compound at 100 cm^{-1} could also be assigned to this mode as observed in Table 6.

4.2.2.1.2. Chromyl group. For chromyl nitrate it is possible to observe two Cr=O stretching modes and four Cr–O stretching modes due to bidentate coordination of the nitrate groups. The scaled DFT frequencies for the Cr=O antisymmetric and symmetric stretching frequencies are in good agreement with the experimental frequencies and normal coordinate calculations. The Cr=O antisymmetric and symmetric stretching modes are easily assigned by comparison with the calculations because in the three cases studied they appear with a higher contribution to P.E.D. and without coupling as shown in Tables 8, S8 and S9. Moreover, in chromyl compounds these modes are observed in 1050–900 cm^{-1} region [44,45,49,51]. The assignment of these modes is similar to the monodentate type as shown in Table 6.

One important observation is that the CrO_2 bending (O=Cr=O) mode appears at higher frequencies than the monodentate type due to four Cr–O bonds: two Cr–O bonds and two Cr ← O bonds (Fig. 5). Hence, it is possible to observe this mode at 475 cm^{-1} with a contribution to P.E.D. of 72% using 6-31G* basis set. In all calculations this mode appears slightly coupled with the Cr–O symmetric stretching. Hence, the shoulder observed in the Raman spectrum at 460 cm^{-1} is assigned to CrO_2 bending (O=Cr=O).

The theoretical calculations predict approximately the Cr–O symmetric stretching mode with the same percentage P.E.D. value (38%) coupled with the CrO_2 deformation and Cr–O antisymmetric stretching modes. The antisymmetric mode is calculated at lower frequencies and both modes with approximately the same contribution (44%). The symmetric mode calculated with higher intensity Raman was assigned to the intense band observed in the Raman spectrum at 446 cm^{-1} while the corresponding antisymmetric stretching was assigned to the weak band observed in the infrared spectrum of the liquid compound at 349 cm^{-1}.

The antisymmetric and symmetric Cr ← O stretchings are obviously calculated at lower frequencies because bond lengths are greater than the Cr–O bonds (see Table 5). It is possible to observe the symmetric mode with higher contribution to P.E.D. at 112 cm^{-1} (26%) with 6-31G* basis set. The antisymmetric stretchings are observed with lower contribution (25%) mixed with other vibration modes at higher frequencies (453 cm^{-1}) with 6-31G* basis set. We assigned these modes in accordance to a higher contribution; i.e. at 206 and 100 cm^{-1} the higher frequency correspond to the antisymmetric stretchings.

In all calculations it is possible to observe the wagging, rocking and twisting modes of the CrO_2 group strongly mixed with other modes. Differently from the monodentate type, the CrO_2 wagging mode is calculated, using 6-31G* basis set, at a lower frequency but, with higher contribution to P.E.D. (247 cm^{-1}, 42% P.E.D.), while the opposite occurs for the CrO_2 rocking mode (calculated at 274 cm^{-1} (34%) with 6-31G* basis set). In this case, the shoulders observed at 247 and 223 cm^{-1} in the infrared spectrum of the liquid chromyl nitrate are assigned to CrO_2 rocking and wagging modes, respectively.

The P.E.D. values indicate that the CrO_2 twisting mode are strongly coupled with vibrations of the same CrO_2 group and NO_2 groups with the 6-31G* basis set. In our case this mode is assigned to 152 cm^{-1}.

4.2.2.2. Nitrate groups as rings of four members. Also, in the bidentate type the calculations were performed with the three basis sets considering the two nitrate groups as a ring of four members where the deformations and torsion coordinates of these groups have been defined as proposed by Fogarasi and Pulay [31] and are observed in Table 3. The frequencies, infrared intensities, Raman activities and potential energy

distribution obtained by B3LYP/6-31G*, B3LYP/Lanl2DZ and B3LYP/6-311+G calculations, appear in Tables 9, S10 and S11, respectively. In all cases the comparison of the theoretical values with the respective experimental values are observed in the respective tables. The calculated harmonic force field for chromyl nitrate can be obtained upon request. Although the best results are obtained with a B3LYP/Lanl2DZ calculation with a RMSD final equal at 12.5 cm^{-1}, the assignment was performed with B3LYP/6-31G* method because the vibration modes appear more defined. In this case a notable change in the assignment, in relation to the above bidentate considerations, is observed.

4.2.2.2.1. Nitrate group. As shown in Table 6, the assignment of the two N=O and NO_2 antisymmetric stretchings not change in reference to the above bidentate type. It is possible to observe some differences only in the frequencies of the two NO_2 symmetric modes. In this case, these modes appear at higher frequencies than the NO_2 deformation modes and the two N=O out of plane deformation modes are observed at lower frequencies. These last modes are assigned to the same frequencies as in the above case while the N=O torsion and two NO_2 torsion modes (out of phase and in phase) are observed in the lower frequencies region, as shown in Table 6.

4.2.2.2.2. Chromyl group. For this group the calculations predict the two Cr=O stretchings, the CrO_2 bending and the four Cr–O stretching modes at the same frequencies as the above bidentate coordination The only change is calculated for the wagging, rocking and twisting modes. In the lower region the A modes are calculated with the two basis sets strongly mixed while in the two bidentate coordinations of the B modes are calculated coupled between them.

For this analysis we think that the two bidentate coordinations are possible but, not the monodentate type because the Cr–O symmetric stretching modes should be observed with higher intensity than the CrO_2 bending mode. Moreover, as we will observe next, the force constants of the Cr–O stretchings cannot be bigger than the corresponding to Cr=O stretchings.

5. Force field

Having a secure assignment for the experimentally studied chromyl nitrate, the corresponding force constants were estimated using the scaling procedure of Pulay et al. [28], as mentioned before. The harmonic force fields in Cartesian coordinates were transformed to the local symmetry or "natural" coordinates proposed by Fogarasi and Pulay [31], as defined in Tables 1–3 (see Figs. 4 and 5) considering in the first case the mode of coordination adopted by nitrate groups as monodentate and in the two following cases as bidentate. The scaling factors affecting the main force constants were subsequently calculated by an iterative procedure [29,30] to have the best possible fit between observed and theoretical frequencies. The resulting numbers for the three cases considered are collected in Table 10. These values are quite satisfactory, considering that the experimental frequencies were not corrected for anharmonicity. The frequencies, infrared intensities, Raman activities and potential energy distribution obtained for chromyl nitrate appear together with the values reached for the corresponding RMSD values in Tables 7–9 and Tables S6–S11 of the Supporting Material, for the three basis sets and for the three coordination modes considered for the nitrate groups in the compound. The force constants appearing in Table 11 expressed in terms of simple valence internal coordinates were calculated from the corresponding scaled force fields by using the expression: $F_i = U^t F_s U$, where F_i is the force constants matrix in terms of simple valence internal coordinates, F_s the force constant matrix in terms of natural coordinates, U the orthogonal matrix relating the natural coordinates to the simple valence

Table 10
Scale factors for the force field of chromyl nitrate

Coordinates	Chromyl nitrate[a]								
	Monodentate			Bidentate			Bidentate[b]		
	Lanl2DZ	6-31G*	6-311++G	Lanl2DZ	6-31G*	6-311++G	Lanl2DZ	6-31G*	6-311++G
ν(N=O)	1.702	0.641	0.825	1.147	0.899	1.137	1.128	0.913	1.075
ν(N-O)	0.798	0.641	0.825	1.147	0.899	1.137	1.128	0.771	0.956
ν(Cr=O)	0.774	0.730	0.815	0.774	0.728	0.816	0.774	0.733	0.815
ν(Cr-O)	1.406	1.029	1.426	1.118	0.908	1.061	1.116	0.950	0.979
δ(O=N=O)	1.090	0.968	1.055				–	–	–
δ(O–N–O)				1.255	1.041	1.248	1.363	1.050	1.397
δ(O=N–O)	1.090	0.968	1.055	1.255	1.041	1.248	1.363	1.050	1.397
δ(O=Cr=O)	1.117	0.917	0.942	1.063	0.941	1.083	0.962	0.906	1.002
δ(O–Cr–O)	1.117	0.917	0.942	1.063	0.941	1.083	1.029	0.941	1.083
δ(O–N–Cr)	1.117	0.917	0.942				–	–	–
τ(O–N–O)	1.034	1.006	1.054	0.984	0.988	0.999	0.946	0.941	1.083
γ(N=O)	1.302	1.002	1.185	1.254	0.999	1.159	1.316	1.008	1.158
ρ(O–Cr–O)	0.861	0.791	0.913	0.785	0.854	0.825	0.946	0.941	1.083
wagg (O–Cr–O)	0.861	0.791	0.913	0.785	0.854	0.825	0.946	0.941	1.083
τw(O–Cr–O)	0.861	0.791	0.913	0.785	0.988	0.999	0.946	0.941	1.083

ν, stretching; δ, deformation; ρ, rocking; wag, (γ) wagging; τw, torsion.
[a] This work.
[b] Considering the nitrate group as ring of four members.

Table 11
Comparison of scaled internal force constants for chromyl nitrate

Coordinates	Chromyl nitrate[a]								
	Monodentate			Bidentate			Bidentate[b]		
	Lanl2DZ	6-31G*	6-311++G	Lanl2DZ	6-31G*	6-311++G	Lanl2DZ	6-31G*	6-311++G
f(N=O)	16.18	16.25	15.83	11.74	11.44	11.71	11.55	11.62	11.07
f(N-O)	3.19	3.38	3.22	4.62	4.96	4.62	4.96	4.96	4.62
f(Cr=O)	6.55	6.55	6.56	6.55	6.53	6.57	6.55	6.57	6.56
f(Cr-O)	7.82	6.09	7.34	1.64	1.44	1.51	1.34	1.38	1.27
f(O=N=O)	1.57	1.62	1.58	–	–	–	–	–	–
f(O=N–O)	2.05	2.24	2.09	1.83	1.74	1.87	1.49	1.32	1.57
f(O=Cr=O)	2.31	2.53	2.26	1.73	1.66	1.74	1.58	1.62	1.63
f(O–Cr–O)	0.86	0.80	0.74	0.91	0.93	0.93	0.75	0.65	0.66
f(O–N–Cr)	1.96	2.41	1.96	–	–	–	–	–	–
f(N=O)/(N–O)	1.74	1.81	1.71	1.33	1.29	1.25	1.66	1.95	1.60
f(N=O)/(Cr–O)	1.16	1.16	1.16	−0.12	−0.07	−0.11	−0.27	−0.47	−0.39
f(N–O)/(N–O)	2.00	2.06	2.09	−1.30	−1.29	−1.29	−1.35	−1.61	−1.36

Units are mdyn $Å^{-1}$ for stretching and stretching/stretching interaction and mdyn Å rad^{-2} for angle deformations.
[a] This work.
[b] Considering the nitrate groups as ring of four members.

internal coordinates, and U^t is the transposed matrix of the U matrix.

It is interesting to compare the principal force constants calculated at the B3LYP/Lanl2DZ, B3LYP/6-31G* and B3LYP/6-311++G levels for the common vibrations, which were collected in Table 11. In general, the calculated force constants values for the two bidentate coordinations considered here, with the B3LYP/Lanl2DZ method are approximately the same as the calculated by B3LYP/6-311++G calculation. Obviously, some force constants values vary when the coordination mode of the nitrate group changes. As expected, the force constants of the N=O and Cr–O stretching change with the coordination mode of the nitrate group, being greater in the monodentate coordination than in the bidentate coordination. The force constants of Cr=O and O–Cr–O deformation modes are practically the same in the two cases, while other modes change as the coordination modes of the nitrate groups change. In CrO_2F_2 and CrO_2Cl_2, the scaled GVFF force constants (B3LYP/Lanl2DZ method) for the Cr=O stretchings are 7.443 and 7.122 mdyn $Å^{-1}$, respectively, while the corresponding force constants for the O=Cr=O deformations are 1.110 and 0.938 mdyn Å rad^{-2} [19]. This difference in the force constant values in reference to chromyl nitrate cannot be attributed to geometrical parameters because they are practically the same in the three compounds. The corresponding values are lower in CrO_2F_2 and CrO_2Cl_2 because the scaled Cr=O frequencies (1015 and 990 cm^{-1}) are higher than the values for $CrO_2(NO_3)_2$ as shown in Tables 7–9. The lower values of the force constants of O=Cr=O deformations in CrO_2F_2 and CrO_2Cl_2 in comparison with the corresponding to $CrO_2(NO_3)_2$ can also be attributed to the scaled O=Cr=O frequencies that are higher in this last compound.

The force constants of Cr–O stretchings considering bidentate nitrate groups are near the expected value reported by Hester and Grossman [53] for an M–O frequency (321 cm^{-1} in bidentate nitrate; 2.0 mdyn $Å^{-1}$). The greater value for this force constant (about 7.82 mdyn $Å^{-1}$) in the monodentate type suggests that the monodentate coordination for the nitrate groups in chromyl nitrate is impossible; therefore, this compound would have multiple coordination.

When the nitrate coordination is monodentate the force constants of N=O stretchings are higher than other coordination modes while in the bidentate type the force constants of the N-O stretchings are higher than the monodentate type. Moreover, our values for the force constants N=O stretching are agree with that the reported value of 11.83 mdyn $Å^{-1}$ for N_2O compound [9] while it is different from the 14.51 mdyn $Å^{-1}$ value reported for the N_2O_2 compound [9]. The structures of both compounds are different from chromyl nitrate, being N_2O linear and N_2O_2 angular with a 90° O–N–N angle. The force constant values reported for KNO_3 by Beattie et al. [52] were: 9.26 mdyn $Å^{-1}$ for N=O stretching; 6.72 mdyn $Å^{-1}$ for N–O stretching; 1.54 mdyn Å rad^{-2} for O–N–O deformation and 1.54 mdyn Å rad^{-2} for O=N–O deformation. The force constant values reported by Brintzinger and Hester [54] for the free anion (6.35 mdyn $Å^{-1}$ for N–O stretching; 2.05 mdyn $Å^{-1}$ for N–O/N–O stretching and 0.54 mdyn Å rad^{-2} for O–N–O deformation) are near the cited values by Topping for D_{3h} nitrate ion (6.5 mdyn $Å^{-1}$ for N–O stretching; 2.05 mdyn $Å^{-1}$ for N–O/N–O stretching and 0.54 mdyn Å rad^{-2} for O–N–O deformation) [55]. For chromyl nitrate, those force constant values for the bidentate type are near to monodentate coordination as can be seen in Table 11. The observed differences in the force constants for KNO_3 can be attributed to the calculations because in that compound they were carried out using three observed N–O stretching frequencies (1460, 1293 and 1031 cm^{-1}) and the C_{2v} bidentate model. The interaction force constants N=O/N–O for the monodentate type in chromyl nitrate are slightly higher than the 1.11 mdyn $Å^{-1}$ value reported for bidentate KNO_3 [53] but close to the obtained values considering the nitrate groups in chromyl nitrate as bidentate.

The analysis of the force constants suggest that the coordination that better represents the group nitrate in chromyl nitrate is the bidentate because the obtained values for this case agree with the one reported by literature values for this coordination mode.

6. Conclusions

In the present paper an approximate normal coordinate analysis, considering the mode of coordination adopted by nitrate groups as monodentate and bidentate, was proposed for chromyl nitrate.

The assignments previously made [1] was corrected and completed in accordance with the present theoretical results. The assignments of the 27 normal modes of vibration corresponding to chromyl nitrate are reported.

The method that best reproduces the experimental vibrational frequencies, considering the two coordination types of the nitrate groups for chromyl nitrate, it is the B3LYP/6-31G*.

The NBO and AIM analysis confirm the hexacoordination of the Cr atom in chromyl nitrate.

We have employed the Lanl2DZ, 6-31G* and 6-311+G basis sets at the B3LYP level to obtain a molecular force field and vibrational frequencies.

An SQM force field was obtained for chromyl nitrate after adjusting the theoretically obtained force constants in order to minimize the difference between observed and calculated frequencies.

We demonstrate that a DFT molecular force field for the chromyl nitrate with the coordination mode adopted by nitrate groups as bidentate, computed using Lanl2DZ, 6-31G* and 6-311+G basis sets are well represented.

Acknowledgements

This work was founded with grants from CIUNT (Consejo de Investigaciones, Universidad Nacional de Tucumán), and CONICET (Consejo Nacional de Investigaciones Científicas y Técnicas, R. Argentina). The authors thank Prof. Tom Sundius for his permission to use MOLVIB and Prof. J. J. López González for the AIM program.

Appendix A. Supplementary data

Supplementary data associated with this article can be found, in the online version, at doi:10.1016/j.saa.2007.06.020.

References

[1] E.L. Varetti, S.A. Brandán, A. Ben Altabef, Vib. Spectros. 5 (1993) 219.
[2] S.A. Brandán, A. Ben Altabef, E.L. Varetti, Spectrochim. Acta 51A (1995) 669.
[3] M. Fernández Gómez, A. Navarro, S.A. Brandán, C. Socolsky, A. Ben Altabef, E.L. Varetti, J. Mol. Struct. (THEOCHEM) 626 (2003) 101.
[4] C. Socolsky, S.A. Brandán, A. Ben Altabef, E.L. Varetti, J. Mol. Struct. (THEOCHEM) 672 (2004) 45.
[5] M.L. Roldán, H. Lanús, S.A. Brandán, J.J. López, E.L. Varetti, A. Ben Altabef, J. Argent. Chem. Soc. 92 (2004) 53.
[6] M.L. Roldán, S.A. Brandán, E.L. Varetti, A. Ben Altabef, Z. Anorg. Allg. Chem. 632 (2006) 2495.
[7] (a) C.C. Addison, N. Logan, S.C. Wallwork, C.D. Garner, Q. Rev. Chem. 25 (1971) 289;
(b) C.C. Addison, N. Logan, Adv. Inorg. Chem. Radiochim. 6 (1964) 71;
(c) C.C. Addison, D. Sutton, Prog. Inorg. Chem. 8 (1967) 195.
[8] W.A. Guillory, M.L. Bernstein, J. Chem. Phys. 62 (3) (1975) 1059.
[9] J. Laane y, J.R. Ohlsen, Prog. Inorg. Chem. 27 (1980) 465.
[10] B. Lippert, C.J.L. Lock, B. Rosenberg, M. Zvagulis, Inorg. Chem. 16 (1977) 1525.
[11] A.D. Harris, J.C. Trebellas, H.B. Jonassen, Inorg. Synth. 9 (1967) 83.
[12] C.J. Marsden, K. Hedberg, M.M. Ludwig, G.L. Gard, Inorg. Chem. 30 (1991) 4761.
[13] M. Schmeisser, D. Lutzow, Angew. Chem. 66 (1954) 230.
[14] M. Schmeiser, Z. Angew. Chem. 67 (17–18) (1955) 493.
[15] S.D. Brown, G.L. Gard, Inorg. Chem. 12 (1973) 483.
[16] G. Brauer (Ed.), Handbuch der Preparativen Anorganischen Chemie, Enke, Stuttgart, 1975, p. 1523.
[17] W.H. Hartford, M. Darrin, Chem. Rev. 58 (1958) 1.
[18] J.C. Bailor, H.J. Emeléus, R. Myholm, A.F. Trotman-Dickenson, Comprehensive Inorganic Chemistry, Pergamon Press, 1975, p. 694.
[19] S. Bell, T.J. Dines, J. Phys. Chem. A 104 (2000) 11403.
[20] A.E. Reed, L.A. Curtiss, F. Weinhold, Chem. Rev. 88 (1988) 899.
[21] J.P. Foster, F. Weinhold, J. Am. Chem. Soc. 102 (1980) 7211.
[22] A.E. Reed, F. Weinhold, J. Chem. Phys. 83 (1985) 1736.
[23] R.F.W. Bader, Atoms in Molecules, A Quantum Theory, Oxford University Press, Oxford, 1990, ISBN 0198558651.
[24] M.J. Frisch, G.W. Trucks, H.B. Schlegel, G.E. Scuseria, M.A. Robb, J.R. Cheeseman, J.A. Montgomery Jr., T. Vreven, K.N. Kudin, J.C. Burant, J.M. Millam, S.S. Iyengar, J. Tomasi, V. Barone, B. Mennucci, M. Cossi, G. Scalmani, N. Rega, G.A. Petersson, H. Nakatsuji, M. Hada, M. Ehara, K. Toyota, R. Fukuda, J. Hasegawa, M. Ishida, T. Nakajima, Y. Honda, O. Kitao, H. Nakai, M. Klene, X. Li, J.E. Knox, H.P. Hratchian, J.B. Cross, C. Adamo, J. Jaramillo, R. Gomperts, R.E. Stratmann, O. Yazyev, A.J. Austin, R. Cammi, C. Pomelli, J.W. Ochterski, P.Y. Ayala, K. Morokuma, G.A. Voth, P. Salvador, J.J. Dannenberg, V.G. Zakrzewski, S. Dapprich, A.D. Daniels, M.C. Strain, O. Farkas, D.K. Malick, A.D. Rabuck, K. Raghavachari, J.B. Foresman, J.V. Ortiz, Q. Cui, A.G. Baboul, S. Clifford, J. Cioslowski, B.B. Stefanov, G. Liu, A. Liashenko, P. Piskorz, I. Komaromi, R.L. Martin, D.J. Fox, T. Keith, M.A. Al-Laham, C.Y. Peng, A. Nanayakkara, M. Challacombe, P.M.W. Gill, B. Johnson, W. Chen, M.W. Wong, C. Gonzalez, J.A. Pople, Gaussian 03 Revision B. 01, Gaussian, Inc., Pittsburgh, PA, 2003.
[25] A.B. Nielsen, A.J. Holder, GaussView, User's Reference, GAUSSIAN, Inc., Pittsburgh, PA, USA, 1997–1998.
[26] A.D. Becke, J. Chem. Phys. 98 (1993) 5648.
[27] C. Lee, W. Yang, R.G. Parr, Phys. Rev. B 37 (1988) 785.
[28] P. Pulay, G. Fogarasi, F. Pang, J.E. Boggs, J. Am. Chem. Soc. 101 (10) (1979) 2550.
[29] T. Sundius, J. Mol. Struct. 218 (1990) 321.
[30] T. Sundius, MOLVIB: A Program for Harmonic Force Field Calculation, QCPE Program No. 604, 1991.
[31] G. Fogarasi, P. Pulay, in: J.E. Durig (Ed.), Vibrational Spectra and Structure, vol. 14, Elsevier, Amsterdam, 1985, p. 125.
[32] E.D. Glendening, A.E. Reed, J.E. Carpenter, F. Weinhold, NBO Version 3.1.
[33] AIM2000 designed by, University of Applied Sciences, Bielefeld, Germany.
[34] R.J. Gillespie (Ed.), Molecular Geometry, Van Nostrand-Reinhold, London, 1972.
[35] R.J. Gillespie, I. Bytheway, T.H. Tang, R.F.W. Bader, Inorg. Chem. 35 (1996) 3954.
[36] S. Wojtulewski, S.J. Grabowski, J. Mol. Struct. 621 (2003) 285.
[37] S.J. Grabowski, Monat. für Chem. 133 (2002) 1373.
[38] R.F.W. Bader, J. Phys. Chem. A 102 (1998) 7314.
[39] P.L.A. Popelier, J. Phys. Chem. A 102 (1998) 1873.
[40] U. Koch, P.L.A. Popelier, J. Phys. Chem. 99 (1995) 9747.
[41] G.L. Sosa, N. Peruchena, R.H. Contreras, E.A. Castro, J. Mol. Struct. (THEOCHEM) 401 (1997) 77.

[42] G.L. Sosa, N. Peruchena, R.H. Contreras, E.A. Castro, J. Mol. Struct. (THEOCHEM) 577 (2002) 219.
[43] S. Wojtulewski, S.J. Grabowski, J. Mol. Struct. 645 (2003) 287.
[44] S.A. Brandán, Estudio espectroscópico de Compuestos Inorgánicos Derivados de Metales de Transición, Doctoral Thesis, National University of Tucumán, R. Argentina, 1997.
[45] H. Siebert, Anwendungen der schwingungsspektroskopie in der Anorganische Chemie, Springer-Verlag, 1966, p. 72.
[46] J.R. Ferraro, A. Walker, J. Chem. Phys. 42 (1965) 1273.
[47] J.R. Ferraro, A. Walker, J. Chem. Phys. 42 (4) (1965) 1278.
[48] J.R. Ferraro y, A. Walker, J. Chem. Phys. 45 (2) (1967) 550.
[49] K. Nakamoto, Infrared and Raman Spectra of Inorganic and Coordination Compounds, 5th ed., J. Wiley & Sons, Inc., 1997.
[50] B.O. Field, C.J. Hardy, Q. Rev. 18 (1964) 361.
[51] M. Chaabouni, T. Chausse, J.L. Pascal, J. Potier, J. Chem. Res. 5 (1980) 72.
[52] I.R. Beattie, J.S. Odgen, D.D. Price, J. Chem. Soc. Dalton (1978) 1460.
[53] R.E. Hester, W.E.L. Grossman, Inorg. Chem. 5 (1966) 1308.
[54] H. Brintzinger, R.E. Hester, Inorg. Chem. (1966) 980.
[55] G. Topping, Spectrochim. Acta 21 (1965) 1743.